1992-12

A comparison of ionospheric propagation mode delay predictions from Advanced PROPHET 4.3 with measured data

Nadal, Jose L.

Monterey, California. Naval Postgraduate School

Approved for public release; distribution is unlimited

A Comparison of Ionospheric Propagation Mode Delay Predictions from Advanced PROPHET 4.3 with Measured Data

by

Jose L. Nadal
Lieutenant, Peruvian Air Force
B.S., Peruvian Air Force Academy, 1988

Submitted in partial fulfillment of the
requirements of degree of

MASTER OF SCIENCE IN ELECTRICAL ENGINEERING

from the

NAVAL POSTGRADUATE SCHOOL
December 1992

assified

ty Classification of this page

REPORT DOCUMENTATION PAGE

eport Security Classification: Unclassified		1b Restrictive Markings	
curity Classification Authority		3 Distribution/Availability of Report	
eclassification/Downgrading Schedule		Approved for public release; distribution is unlimited.	
forming Organization Report Number(s)		5 Monitoring Organization Report Number(s)	
ame of Performing Organization al Postgraduate School	6b Office Symbol *(if applicable)* EC	7a Name of Monitoring Organization Naval Postgraduate School	
ddress *(city, state, and ZIP code)* terey CA 93943-5000		7b Address *(city, state, and ZIP code)* Monterey CA 93943-5000	
ame of Funding/Sponsoring Organization	8b Office Symbol *(if applicable)*	9 Procurement Instrument Identification Number	
ddress *(city, state, and ZIP code)*		10 Source of Funding Numbers	
		Program Element No / Project No / Task No / Work Unit Accession N	

tle *(include security classification)* A COMPARISON OF IONOSPHERIC PROPAGATION MODE DELAY PREDICTIONS FROM PROPHET 4.3 H MEASURED DATA

ersonal Author(s) NADAL, Jose L.

Type of Report	13b Time Covered	14 Date of Report *(year, month, day)*	15 Page Count
ter's Thesis	From To	1992 DEC 15	64

pplementary Notation The views expressed in this thesis are those of the author and do not reflect the official policy or position he Department of Defense or the U.S. Government.

osati Codes			18 Subject Terms *(continue on reverse if necessary and identify by block number)*
	Group	Subgroup	High Frequency (HF); Ionospheric Propagation; ADVANCED PROPHET

ostract *(continue on reverse if necessary and identify by block number)*

is thesis compares the outputs of the ionospheric propagation prediction model ADVANCED PROPHET 4.3 to measurements ropagation mode delay for a High Frequency communications link between Monterey and San Diego, California.

ode delay variations throughout the day are presented for experimental data PROPHET predictions. Amargin of error of less 0.5 msec was considered acceptable and the number of acceptable predictions per day was generated. Acceptable predicted collected over the test period was analyzed to establish wish hours of the day PROPHET accurately predicts propagation mod y independent of frequency, date and power levels. During the first six hours of the day PROPHET data tracks experimental for mode delay change patterns. On a daily basis, predictions are best between 1400 and 1700 GMT (0600 and 0900 local), although patterns could not be established for other hours of the day.

edicted mode delay percentage distribution show greater correlation during the first three hours of the morning and at sunset.

stribution/Availability of Abstract nclassified/unlimited __ same as report __ DTIC users	21 Abstract Security Classification Unclassified	
Name of Responsible Individual ard W. Adler	22b Telephone *(include Area Code)* 408-646-2352	22c Office Symbol EC/Ab

FORM 1473,84 MAR 83 APR edition may be used until exhausted

All other editions are obsolete

security classification of this p

Unclassif

ABSTRACT

This thesis compares the outputs of the ionospheric propagation prediction model ADVANCED PROPHET, 4.3 to measurements of propagation mode delay for a High Frequency communications link between Monterey and San Diego, California.

Mode delay variations throughout the day are presented for experimental data and PROPHET predictions. A margin of error of less than 0.5 msec was considered acceptable and the number of acceptable predictions per day was generated. Acceptable predicted data collected over the test period was analyzed to establish which hours of the day PROPHET accurately predicts propagation mode delay, independent of frequency, date and power levels. During the first six hours of the day PROPHET data tracks experimental data for mode delay change patterns. On a daily basis, predictions are best between 1400 and 1700 GMT (0600 and 0900 local time), although patterns could not be established for other hours of the day.

Predicted mode delay percentage distributions show greater correlation during the first three hours of the morning and at sunset.

TABLE OF CONTENTS

LIST OF FIGURES

I. INTRODUCTION

The concept of an electrical conducting layer in the atmosphere dates back to the mid-19th century. Shortly after the invention of radio, when communications distances began to increase, the relation between propagated waves and this electrical layer, now known as the ionosphere was observed. Since then, many studies have been conducted on the characteristics of the ionosphere and its effects on radio communications.

The principal use of the ionosphere is in the High Frequency (HF) band. Since communication in the HF band depends on ionospheric wave reflection, which is continuously changing due to daily, seasonal, and solar conditions, the effect of the changing ionosphere on radio communications must be considered. Ionospheric communication, when reliable, has several advantages over other methods. The low cost, simplicity, and portability of equipment are advantages over other communications methods that may be more reliable. Communications via the ionosphere is wide spread among CIS and third-world countries and is being given consideration as a viable alternative by other users.

It is impossible to maintain reliable communications without considerating the changing environment in which it occurs. Hence, it is important to have knowledge of

ionospheric characteristics and the elements that affect it such as time of day, season, location, and solar activity [1].

Computer models permit the analysis of HF wave propagation parameters and can predict propagation channels that will support communications.

A project named Polar Equatorial Near-Vertical Incidence Skywave Experiment (PENEX) which acquires calibrated field strength measurements from ionospheric radio transmissions is creating a data base for comparison with different ionospheric propagation prediction models. In addition, as part of the PENEX project, a communication link has been established for the purpose of equipment testing, calibration and experimental methodology.

After this communication link between Monterey, CA. and San Diego, CA. is tested, project PENEX will be expanded to include a transmitter site in Alaska, and receiver sites in Alaska, California, Pennsylvania and Washington.

This thesis uses one of the computer models, ADVANCED PROPHET 4.3 to predict HF skywave propagation for comparison and correlation to the experimental data obtained for mode delays in the communication link between Monterey and San Diego.

It is also important to note that due to limited data availability, the research analysis of this thesis is somewhat restricted.

II. THEORETICAL BACKGROUND

A. THE IONOSPHERE

The ionosphere is the region of the atmosphere which extends between 50 to 600 km where sufficient ionization occurs in layers to affect radio transmissions. The ionosphere is an electrically neutral region, since if it had a given excess charge, then electrical forces would prevent the formation of stable layers [2].

1. Photo-ionization

Photo-ionization occurs when the sun produces extreme ultraviolet (EUV) light waves which in turn detach electrons from neutral atoms in the Earth's atmosphere. When this takes place, the atoms become positive ions as illustrated in Figure 1.

Since the atmosphere is bombarded by EUV of different frequencies, different layers are formed at different altitudes; higher frequency EUV waves penetrate the atmosphere deeper, producing layers at lower altitudes while lower frequency EUV penetrates less, producing higher altitude layers [3].

2. Recombination

When collisions are produced between positive ions and free electrons, neutral atoms are formed. Recombination can be seen as the photo-ionization process in reverse.

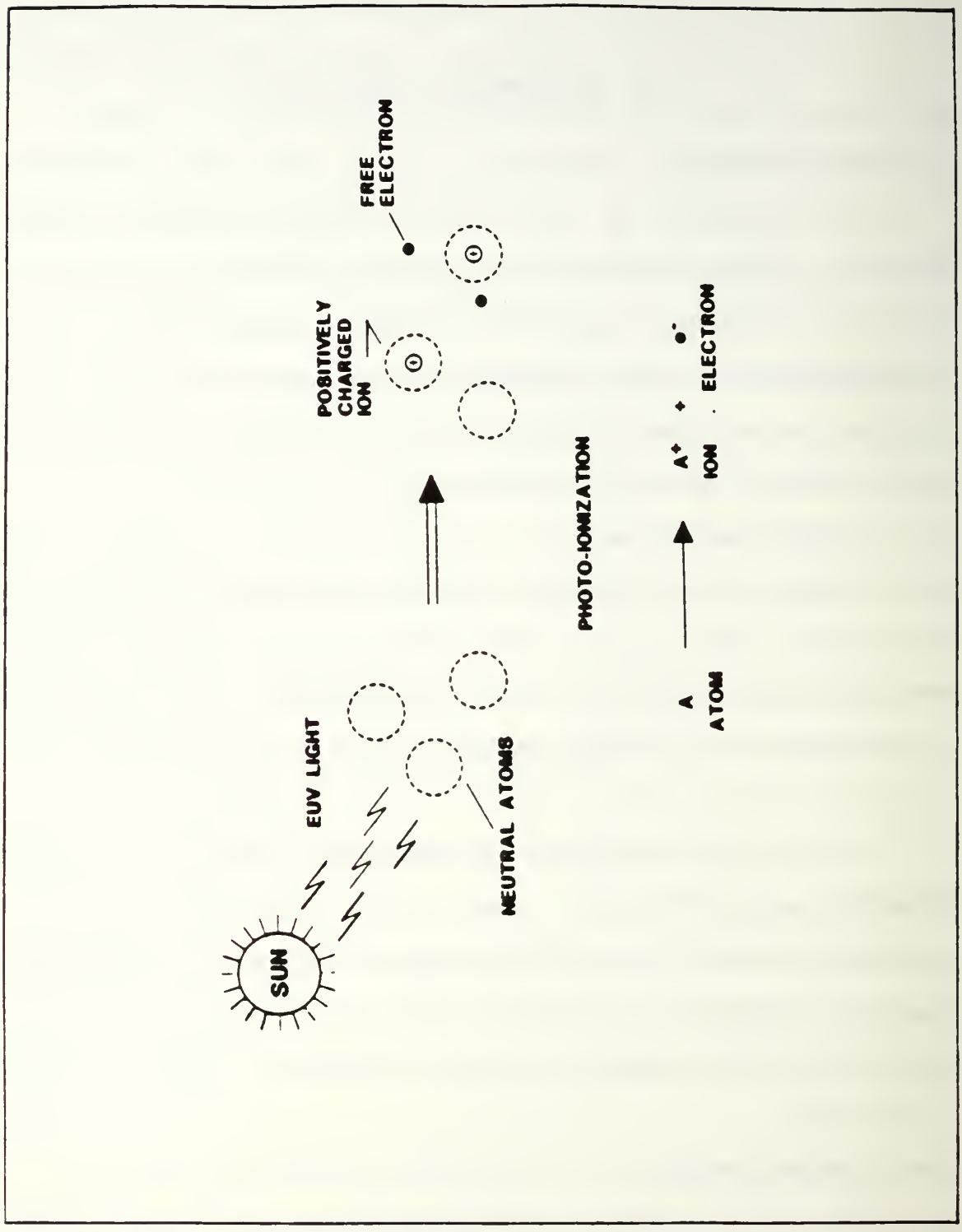

Figure 1. Photo-ionization of a neutral atom, A, by extreme ultraviolet light from the sun, yielding a positively charged ion, A^+, and a free electron, e. [Ref.1, p. 18]

Between dawn and dusk, photo-ionization exceeds recombination and maximum density layers are formed affecting radio communications in greater percentages than during the hours after dusk when the effect is reversed.

3. Ionospheric Layers

The ionosphere divides into three mayor layers, D, E , and F which is sub-divided into two others, F1 and F2.

The lowest layer is the D-layer which spans from 50 to 90 km. In the D-layer low frequency (LF) waves are refracted while Medium Frequency (MF) and High Frequency (HF) waves are absorbed. There are two types of absorption that affect the HF band: deviative and nondeviative. Deviative absorption occurs when the refractive index approaches zero, generally at the apex of the trajectory, while nondeviative absorption takes place when the refractive index approaches one and the product between electron density and electron collision frequency is high [2]. Another aspect of the D-layer is that it disappears after sunset due to rapid recombination.

The E-layer is located between 90 and 130 km and is also known as the "Kenelly-Heaviside layer". This layer is characterized by strong diurnal variations. Recombination is rapid after sunset and the layer diminishes as the night advances. The Sporadic E-layer also occurs near 120 Km and exists throughout the day at lower (equatorial) latitudes and during late night for higher (polar) latitudes. The E-layer reflects signals up to 20 MHz providing communications at

distances up to 2500 km per reflection.

The F-layer is formed between 150 and 600 km. During the daytime this layer divides into two layers, F1 and F2, located between 150 and 220 km and above 225 km, respectively. Since these layers are at the highest altitudes, photo-ionization occurs at the highest rate. At noon time in the northern latitude winter, these layers are the closest to the sun and the ionization rates are maximum. Because the atmospheric density diminishes with altitude, the F-region recombination process is relatively slow and at night the F-layer is always present. Figure 2 shows the different layers of the ionosphere.

4. Variations of the Ionosphere

Since the ionosphere is created by the effect of solar radiation upon the atmosphere, the ionosphere will also vary with the time of the day, season, location on the earth, solar activity, and other similar factors.

These variations that affect the ionosphere will also affect HF communications. The principal variations of the ionosphere are:

* Diurnal (throughout the day)
* Seasonal (throughout the year)
* Location (geographic and geomagnetic)
* Solar Activity (Solar cycle and disturbances)
* Height (different layers) [1]

Figure 3 illustrates how diurnal variations affect the

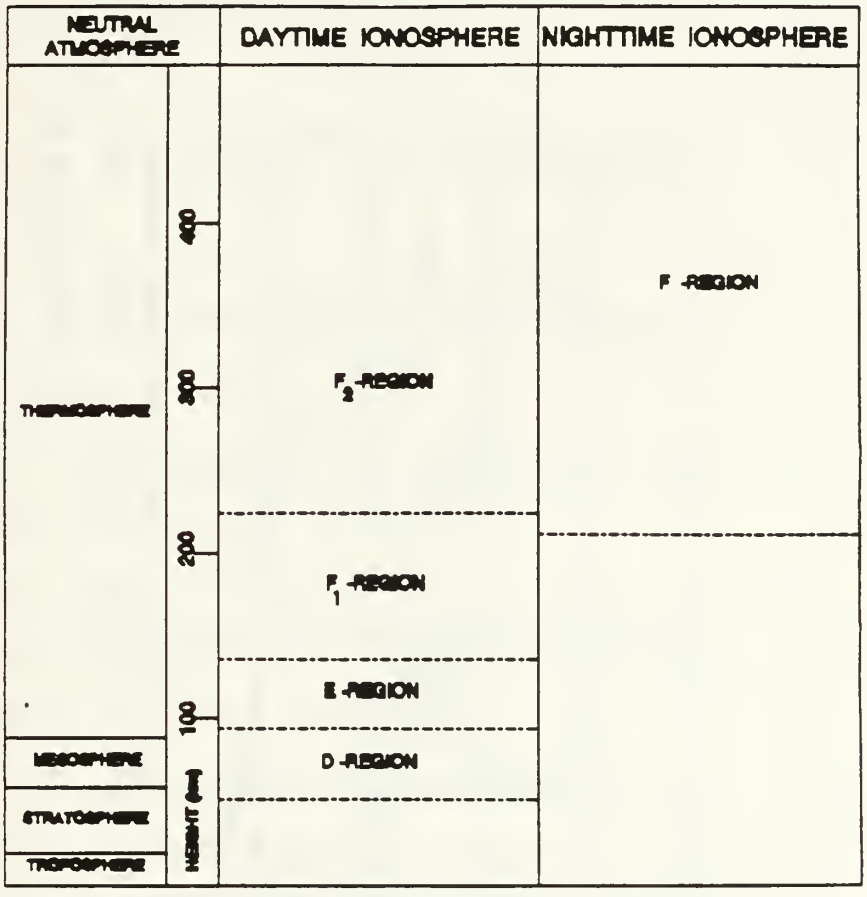

Figure 2. Sketch of the various regions of the ionosphere as it appears during the day and during the night. [Ref.1, p. 17]

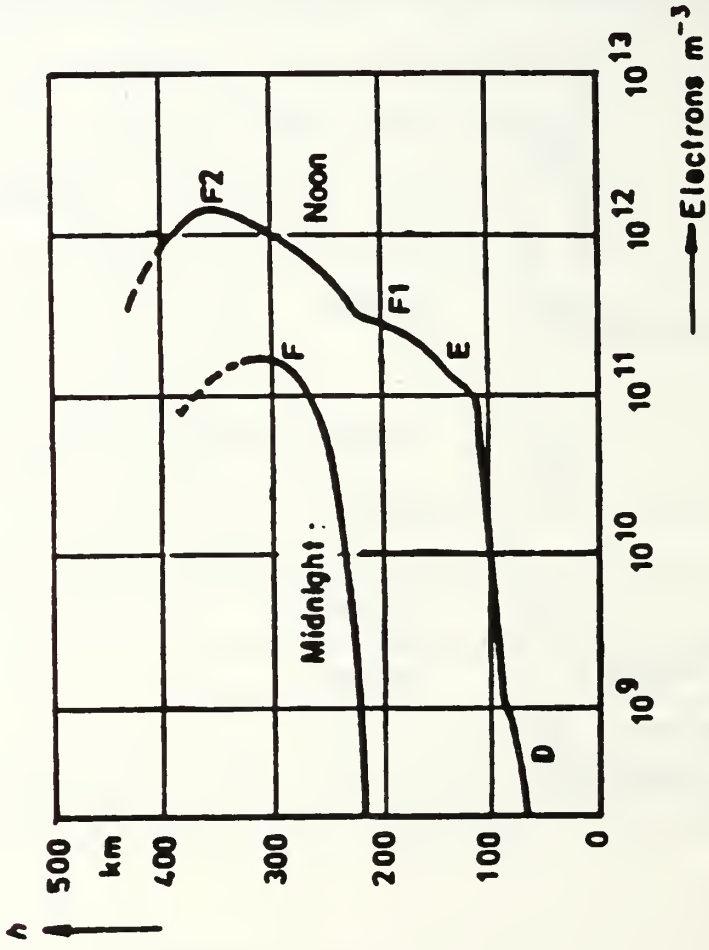

Figure 3. Diurnal variation of electron density and the formation of ionospheric layers. [Ref.6, p. 21]

formation of ionospheric layers.

5. Ray Tracing

In order to determine the amplitude, phase, polarization, flight time, etc. of the transmitted wave, it is necessary to determine the ray path between the transmitter and the receiver. Determining the ray path seems to be a simple task but in practice it is not. Factors affecting the ray path are the orientation and intensity of the earth's magnetic fields, the collision frequency of electrons and electron density variations within the layers. Thus, calculations are much more complex for the real-world than for the assumption that the ionosphere is a homogeneous layer.

6. Ray Paths in the Ionosphere

The path followed by a wave reflected from the ionosphere depends on the incidence angle at the ionosphere. After entering the ionosphere, a wave can take different paths. It could reach the receiver via one hop, i.e., bouncing off the ionosphere once, or through multiple hops. Reflection between the different layers in the ionosphere as well as any combination of the above cases is also a possibility. Figure 4 shows examples of different paths for a wave using the ionosphere.

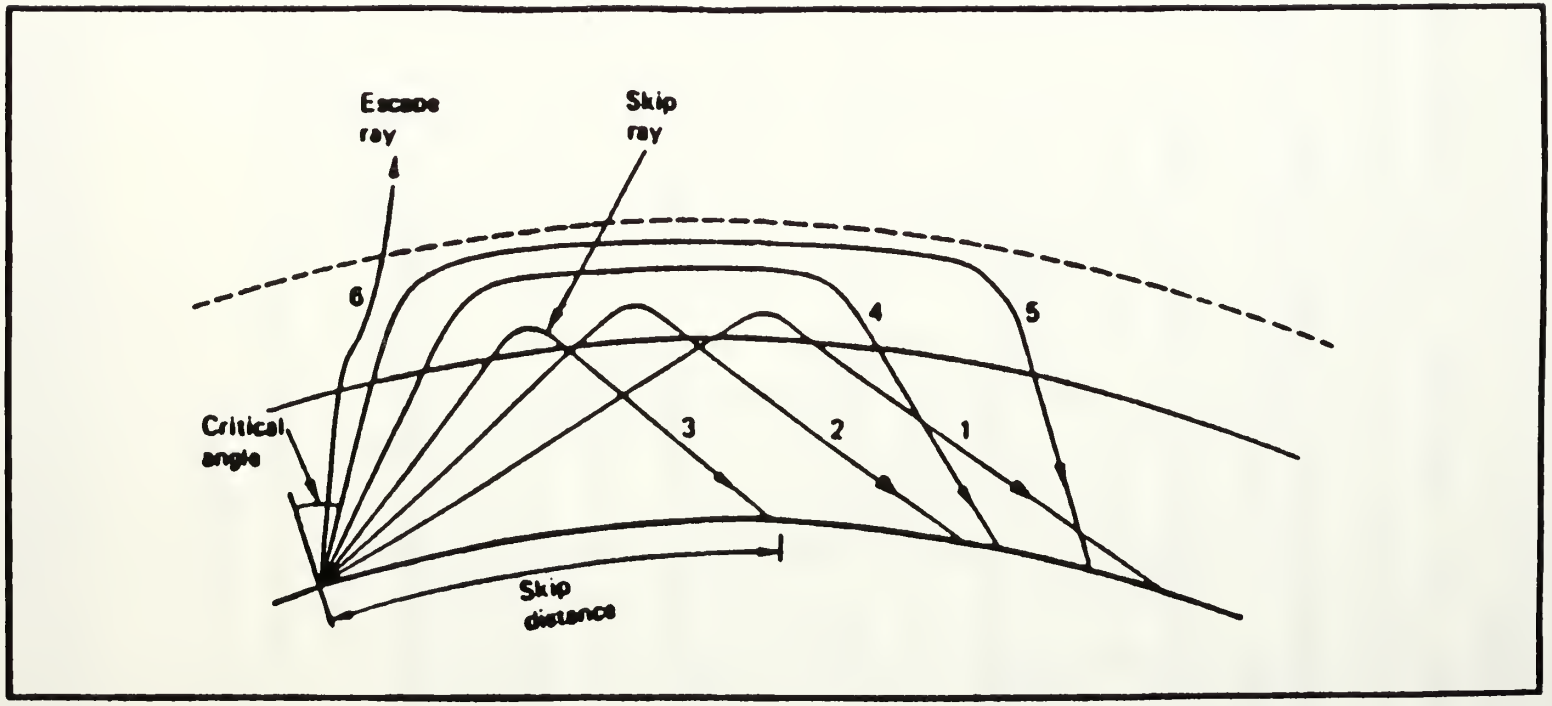

Figure 4. Raypaths for a fixed frequency. [Ref.4, p. 62]

III. THE MONTEREY-SAN DIEGO COMMUNICATION LINK

Before the polar region HF ionospheric communication link for PENEX is installed, a test-bed link was established to verify the operation of the equipment and software. For this link, Monterey was designated as the transmitter site with San Diego as the receiver site. The geographical latitude and longitude used in the scenario files of ADVANCED PROPHET 4.3 are 36°37′ N latitude and 121°55′ W longitude for Monterey and 32°43′ N latitude and 117°09′ W longitude for San Diego. The transmit power for the tests is 2.5, 75 and 100 watts and the frequencies are 5.604 and 11.004 MHz. The methodology of experimentation is described in detail in Chapter IV.

A. LINK ANTENNAS

The description of the antenna characteristics for the transmitter and receiver sites are essential for modeling the skywave propagation and for the link power budgets.

1. Transmitting Antenna

The transmitting antenna utilized is a multiband dipole which consists of a group of three half-wavelength dipoles connected to a common transmission line. The multiband dipole is designed to operate on 5.6, 11 and 16.8 MHz respectively. For data collection purposes the antenna was operated at 5.604 and 11.004 MHz since 16 MHz propagation was very unlikely for the test link. The data collected for the 11.004 MHz

frequency range was obtained for only one day, during the time of this investigation.

Dipole lengths were 5.6, 11, and 16.8 MHz for 24.69, 13.05, and 8.53 meters, respectively. Since these dipoles are center-fed, each has two elements half the dimensions given above. Figure 5 shows the dipole antenna geometry details. The separation between the dipoles is 0.3048 meters and the upper and lower elements are at an elevation angle of 11.21° and -11.21° respectively. The dipoles are fed by a 50 ohm impedance coaxial cable connected to a 1:1 balun transformer.

2. Receiving Antenna

The receiver antenna in San Diego is a dipole, containing three half-wavelength dipoles on one structure, drooping from the center at -34°. It is designed to operate at the same frequencies as the transmitting antenna.

The half lengths of each element are 12.73 m., 6.48 m., and 4.24 meters for frequencies 5.6, 11, and 16.8 MHz respectively. The separation between elements is 12.7 cm and the feed line is a 50 ohm coaxial cable. Figure 6 shows the details of the receiver antenna.

3. Antenna Simulation

The transmit antenna designs were modeled by a Naval Postgraduate School student using the Numerical Electromagnetics Code (NEC) which in turn provided patterns for ADVANCED PROPHET 4.3. Figures 7 and 8 show radiation patterns from NEC. In ADVANCED PROPHET 4.3, these patterns

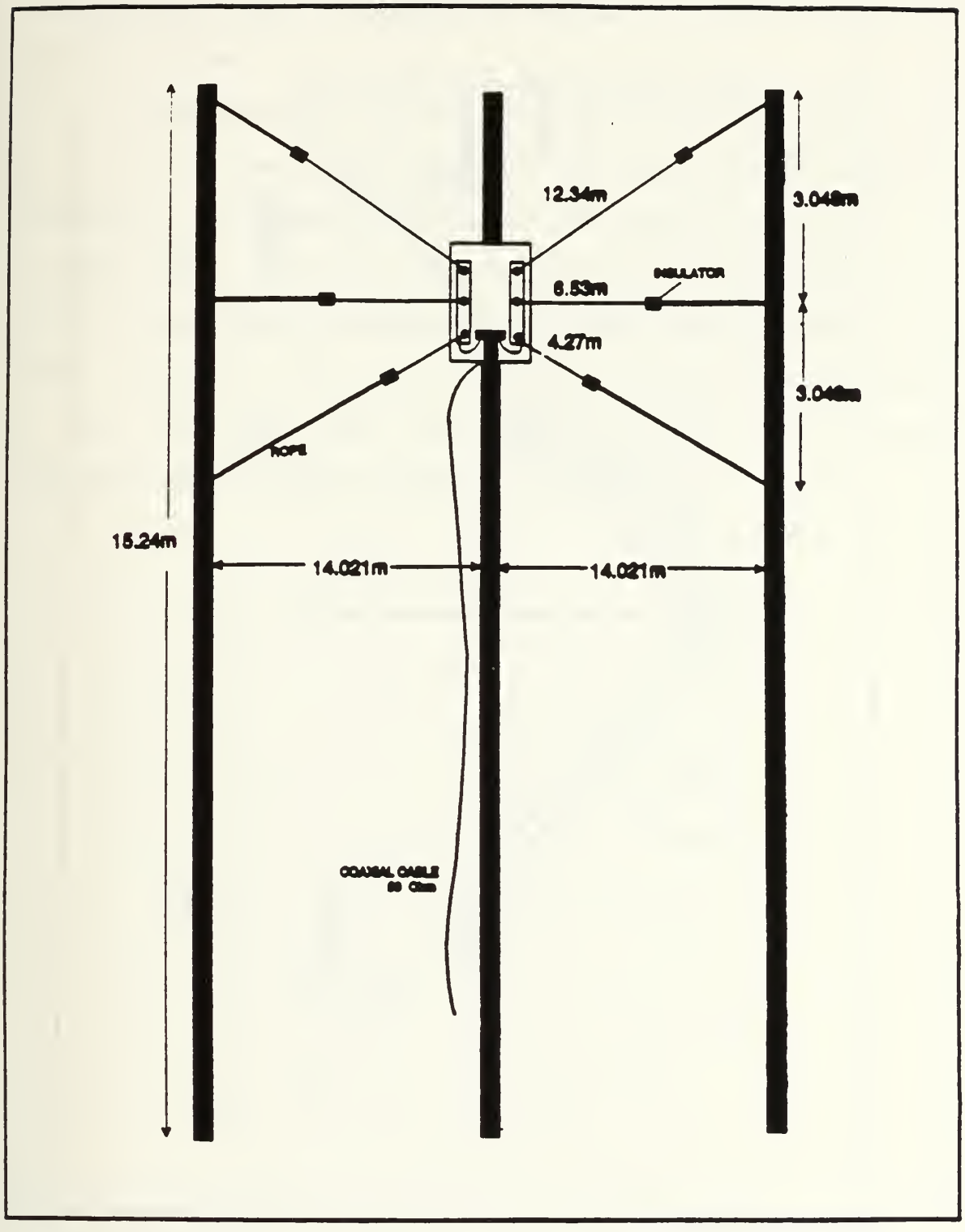

Figure 5. Monterey Multiband Dipole Antenna

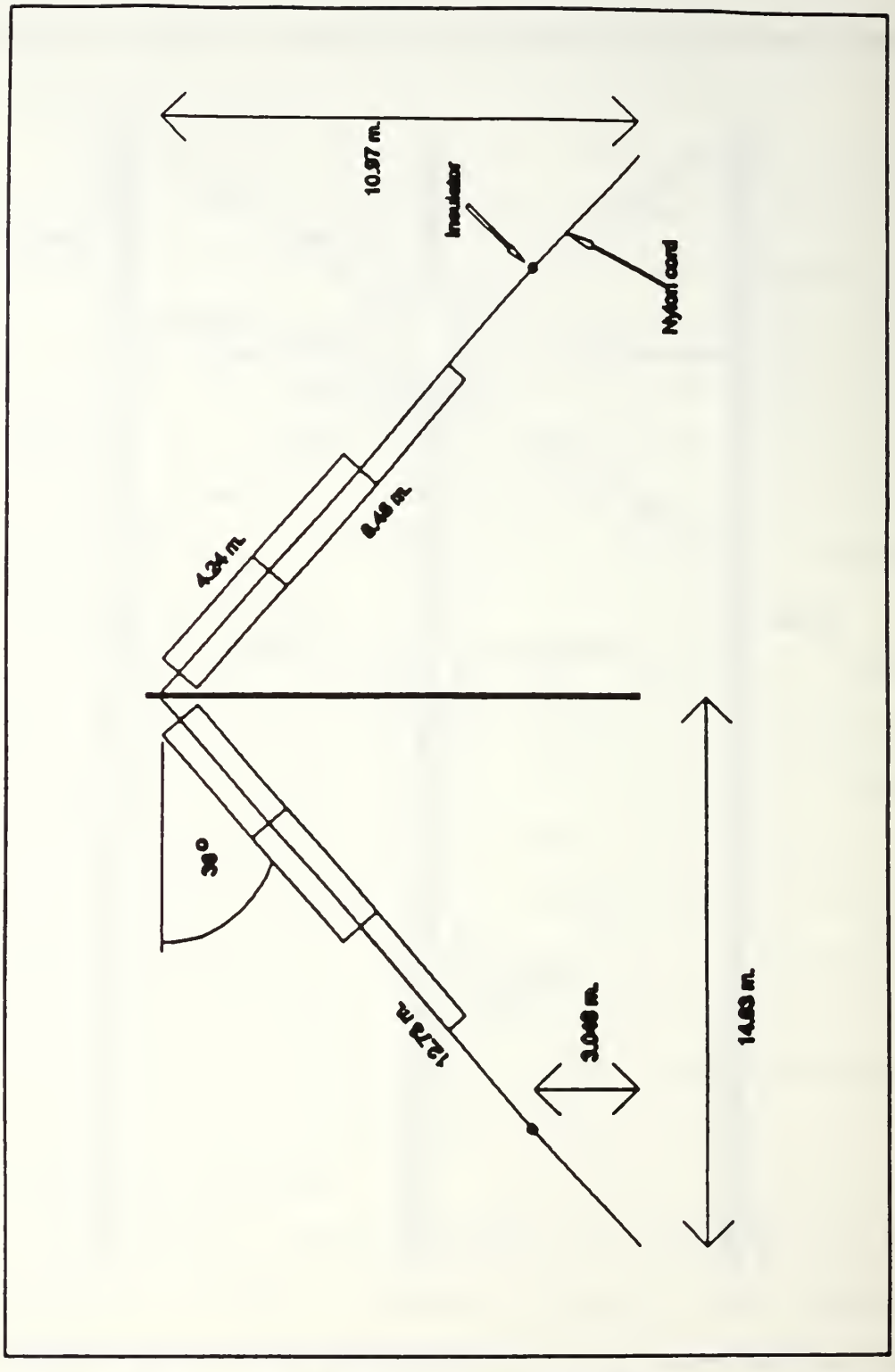

Figure 6. San Diego Drooping Dipole Antenna

are required only for elevation angles of 6, 20, 40, 50, 70, and 90 degrees.

Since radiation pattern definition in ADVANCED PROPHET 4.3 is for the entire HF band and for only integer values of frequency, the pattern for 5.6 MHz was used for 2, 3, 4, 5, 6, 7, and 8 MHz. Likewise, the 11 MHz pattern was used for 9, 10,11,12 and 13 MHz, while the 16.8 MHz radiation pattern was used for 14, 15, 16, 17, 18, 19, 20, 25, and 30 MHz. Figures 9 and 10 show the radiation patterns and antenna characteristics used by ADVANCED PROPHET 4.3.

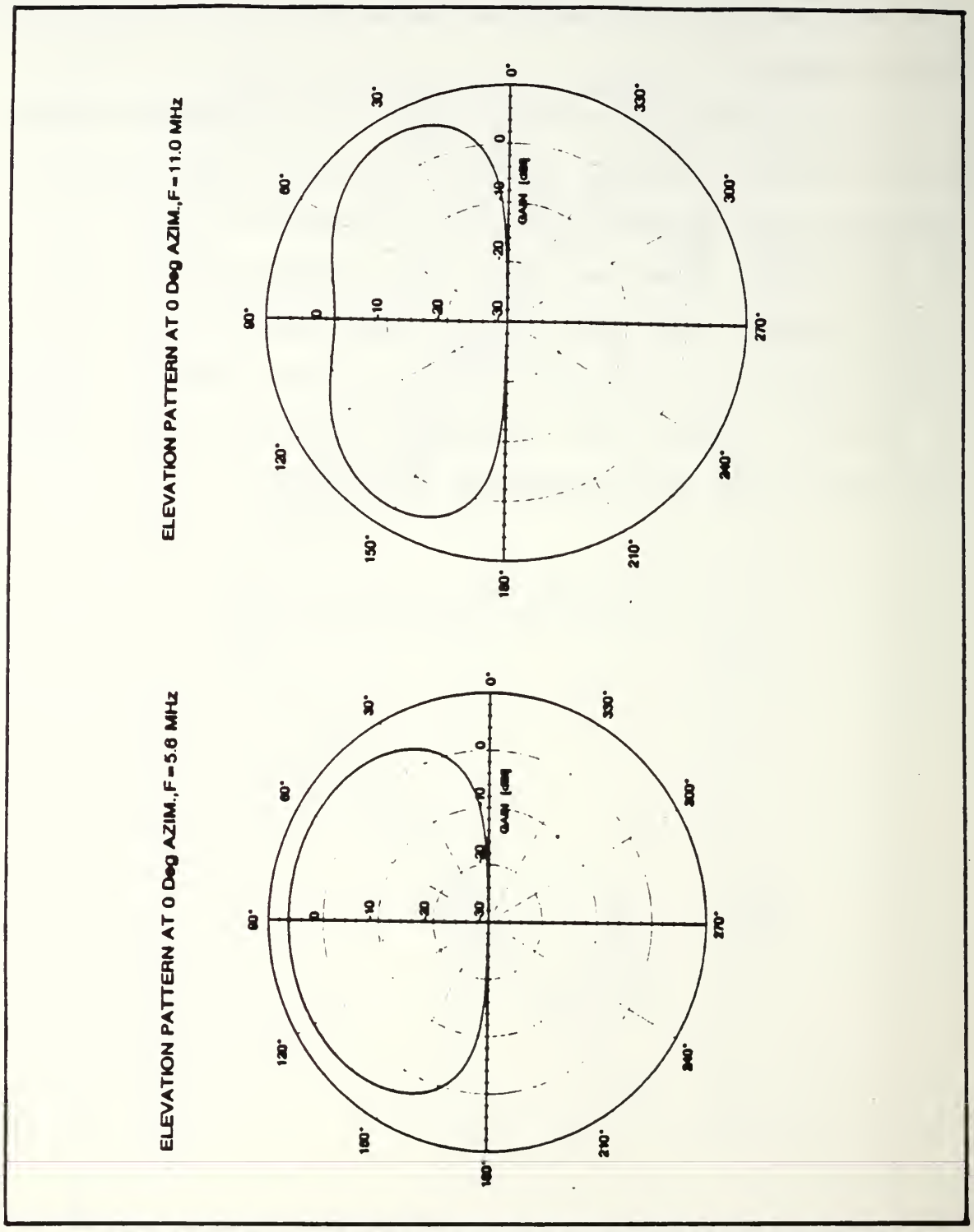

Figure 7. Elevation radiation patterns obtained by NEC for the Multiband Dipole Antenna

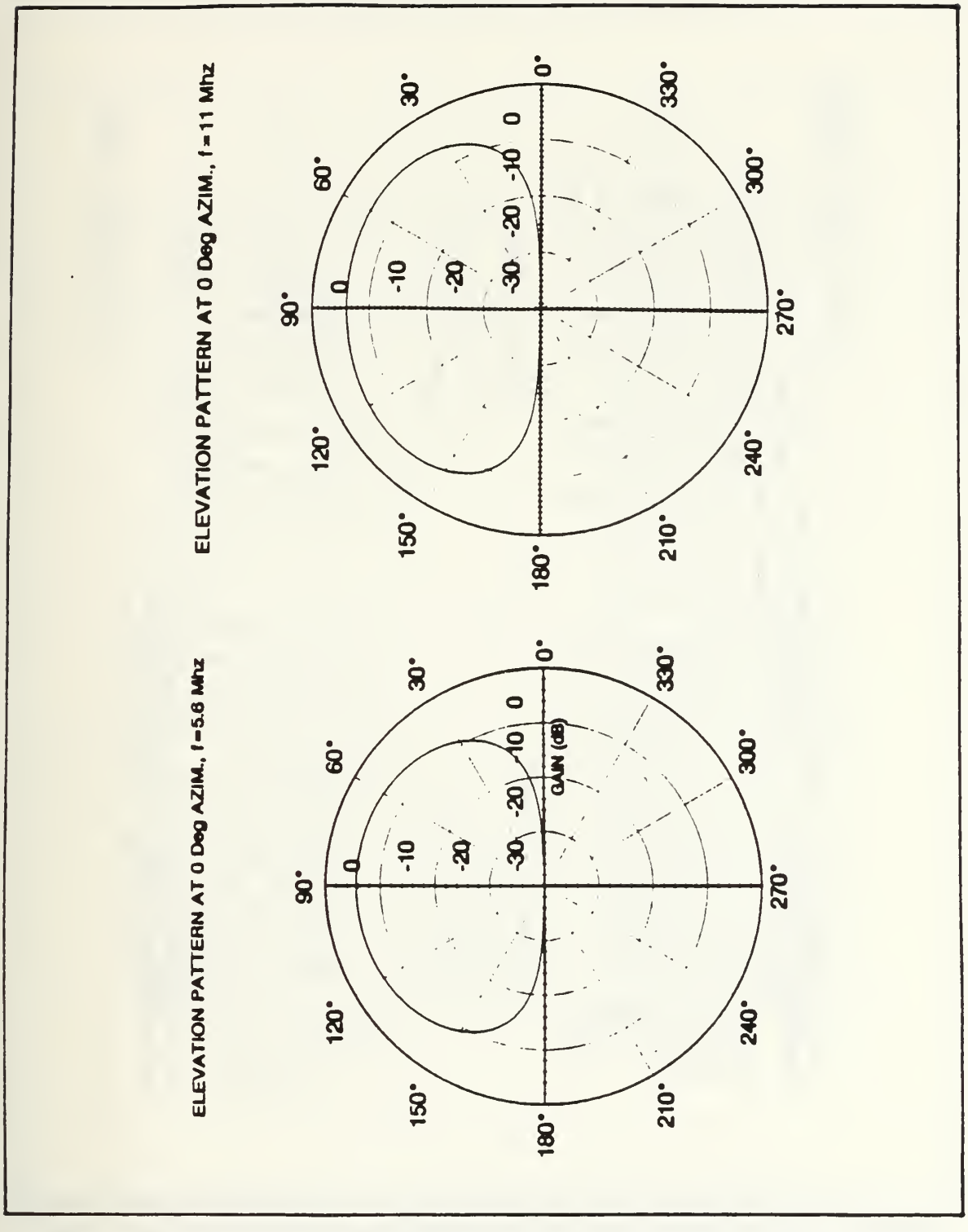

Figure 8. Elevation radiation patterns obtained by NEC for the Drooping Dipole Antenna

Figure 9. Elevation radiation patterns used by PROPHET for the Multiband Dipole Antenna

Figure 10. Elevation radiation patterns used by PROPHET for the Drooping Dipole Antenna

IV. COMPARISON OF EXPERIMENTAL DATA WITH PROPHET PREDICTIONS

A. EXPERIMENTAL DATA

The following data are collected via PENEX equipment and software at the San Diego receiver site. The PENEX system uses direct sequence spread spectrum modulation (DSSS), specifically phase shift keying (PSK), to transmit a reference maximum length sequence. The system measures mode time delay and signal strength using a quadrature-sampled, Fast Fourier Transform (FFT) matched-filter signal processor. The time delay measurements have a 25 millisecond (msec) resolution. This system provides a precise time delay measurement as well as consistent signal strength measurements.

Figure 11 shows an example of correlation vector plots resulting from cross correlation of the reference sequence with the digitized HF data. The upper plot is the raw vector (linear form), of approximately 10 msec of data. Since the digitizing rate is 39.0625 MHz, each bin is 25.6 microseconds. In order to determine the mode delay, delta t, and the value of the correlation peak, this vector is scanned to locate the peaks, record the corresponding correlation peak values, and find the distances between adjacent peaks (in terms of the intervening bin count). The number of intervening bins is then multiplied by the 25.6 microsecond duration of each bin, yielding the mode delay, delta t. Next, the value of the

Figure 11. Correlation vector plot that results from the cross correlation of the reference sequence with the digitized HF data.

correlation peak is mapped, through a calibration curve, to received voltage and later, through the CCIR field strength equation, to field strength. It is important to note that the dB value obtained for all three modes in Figure 11 is not the field strength but rather a processing gain measurement

(20*LOG{max correlation/noise floor}).

The information produced by the PENEX team consists of mode delay vs. real time graphs for five different days, as shown on Table 1; three different transmission power levels and two frequencies were used.

TABLE 1. DATE OF TRANSMISSION, FREQUENCY AND POWER USED BY THE MONTEREY-SAN DIEGO COMMUNICATION LINK.

Date	Frequency (MHz)	Power (watts)
28 Aug 92	5.604	2.50
02 Oct 92	5.604	75.00
03 Oct 92	5.604	75.00
04 Oct 92	5.604	75.00
07 Oct 92	5.604	75.00
02 Oct 92	11.004	100.00

The plots shown in Figures 12 through 17 provide time delay for 24 hours of each day. For the purpose of comparison, the data considered were the data corresponding to each hour interval. All mode delays were stored on file for later comparisons. All times are in GMT, (the Monterey-San Diego Link has a -8 hour offset). Table 2 shows the time

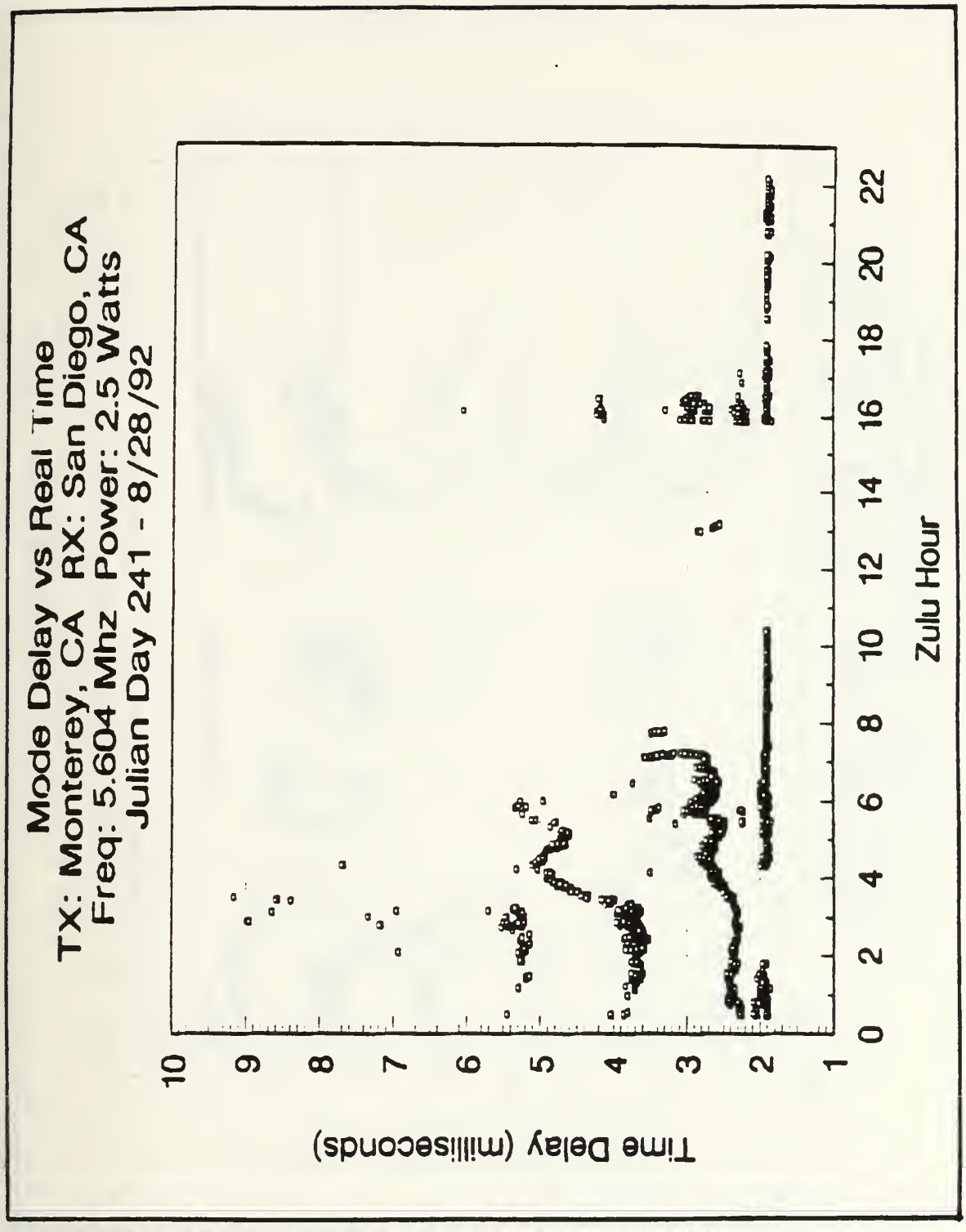

Figure 12. Measured Mode Delay for 28 Aug 92.

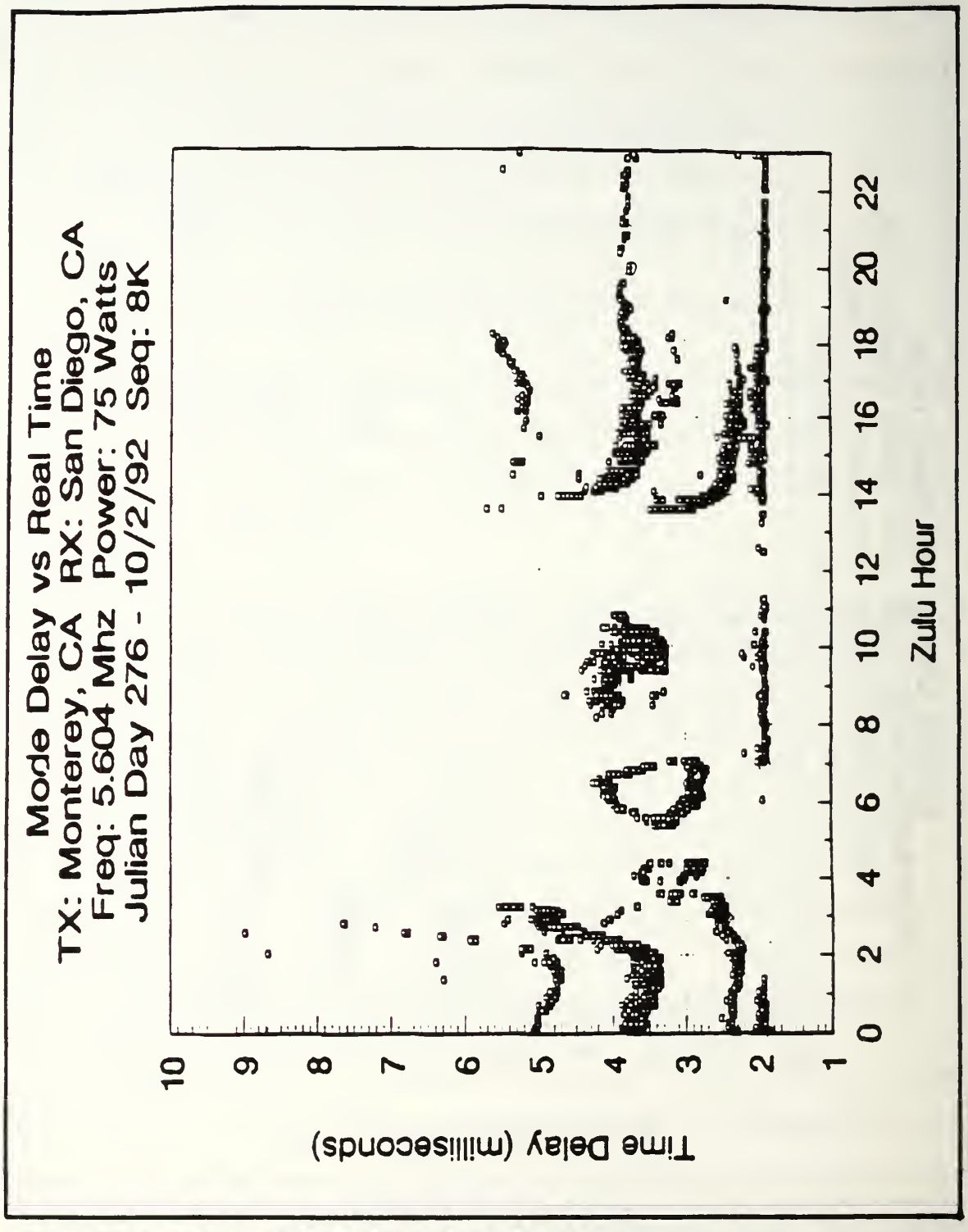

Figure 13. Measured Mode Delay for 2 Oct 92.
(5.604 MHz - 75 watts)

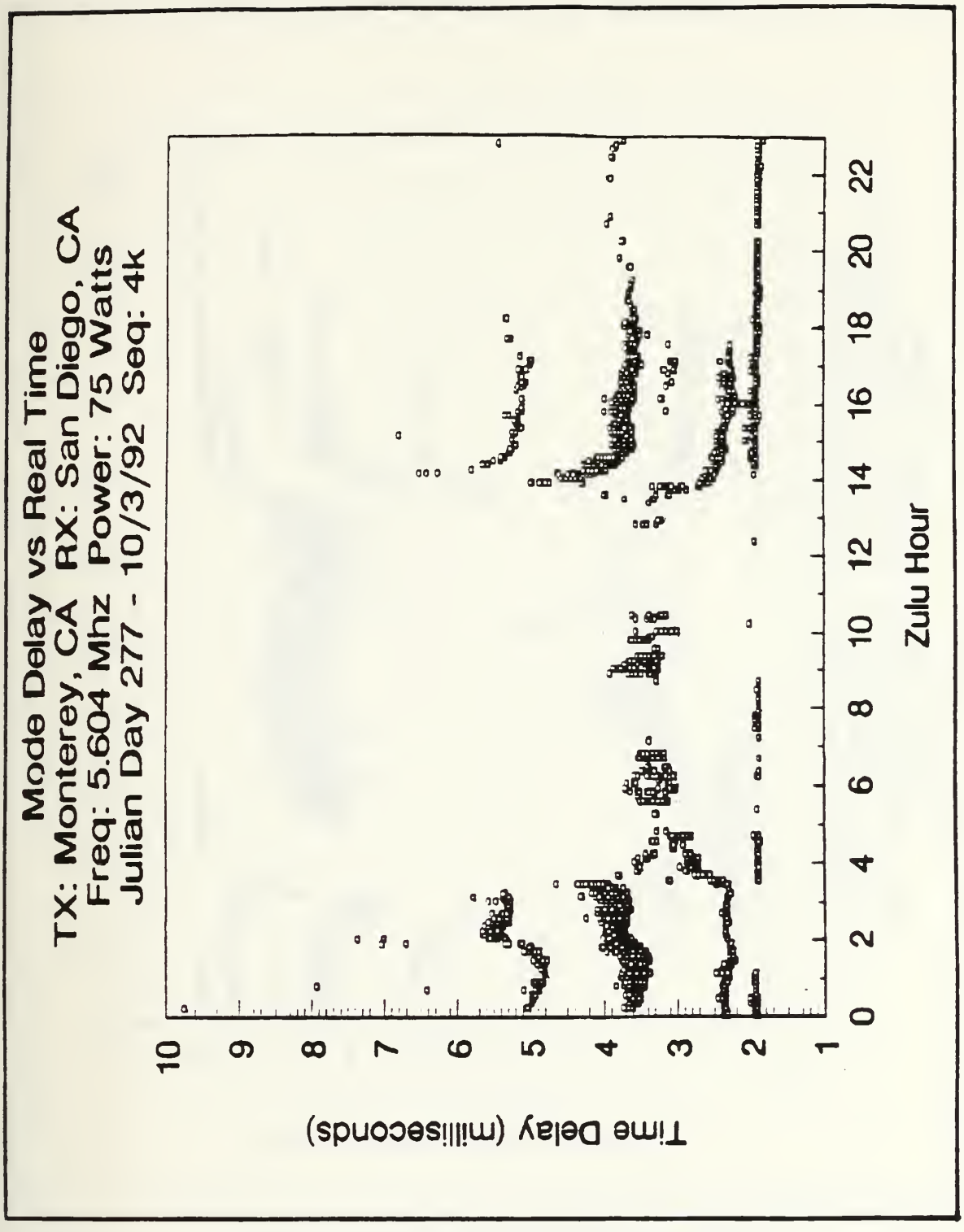

Figure 14. Measured Mode Delay for 3 Oct 92.

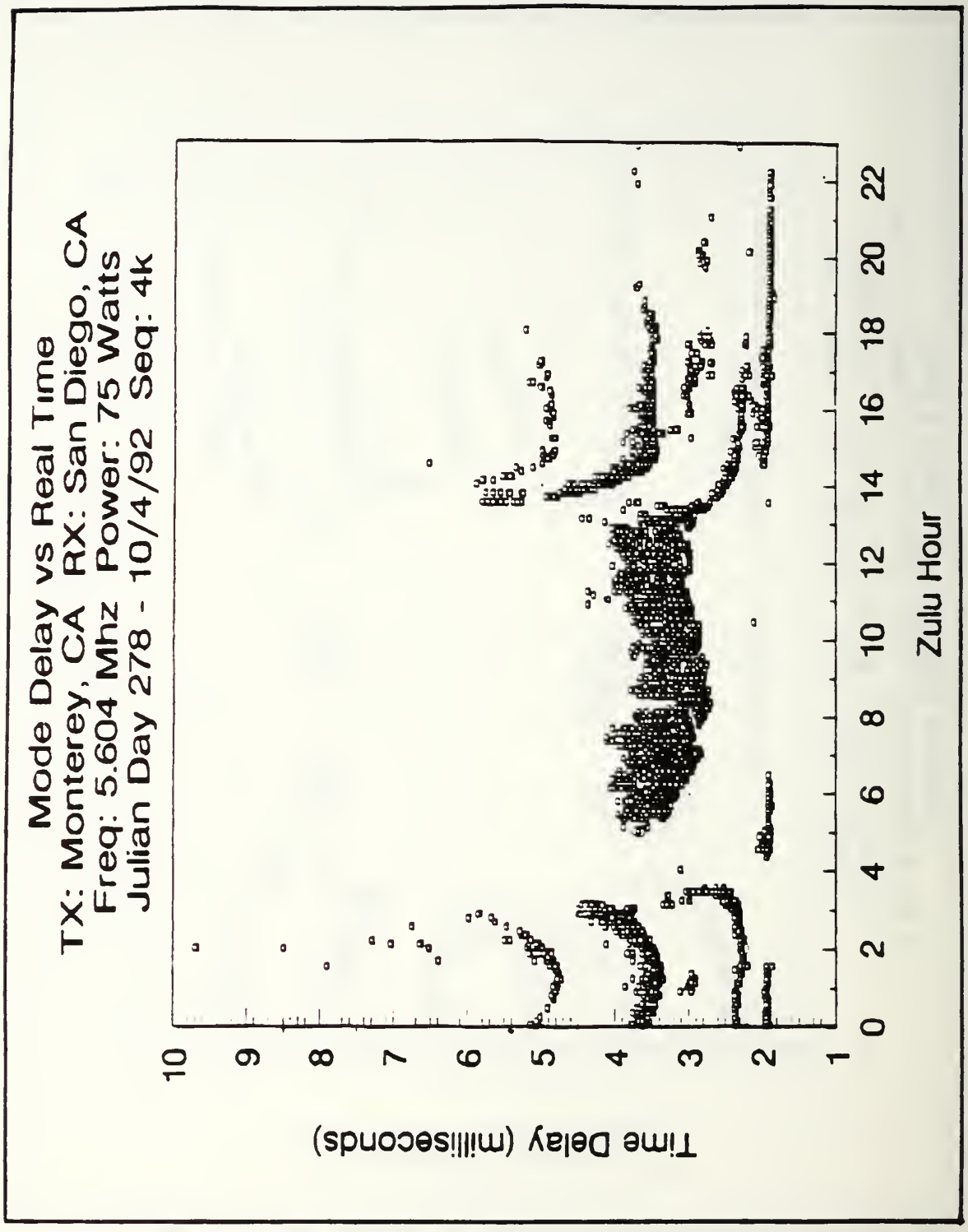

Figure 15. Measured Mode Delay for 4 Oct 92.

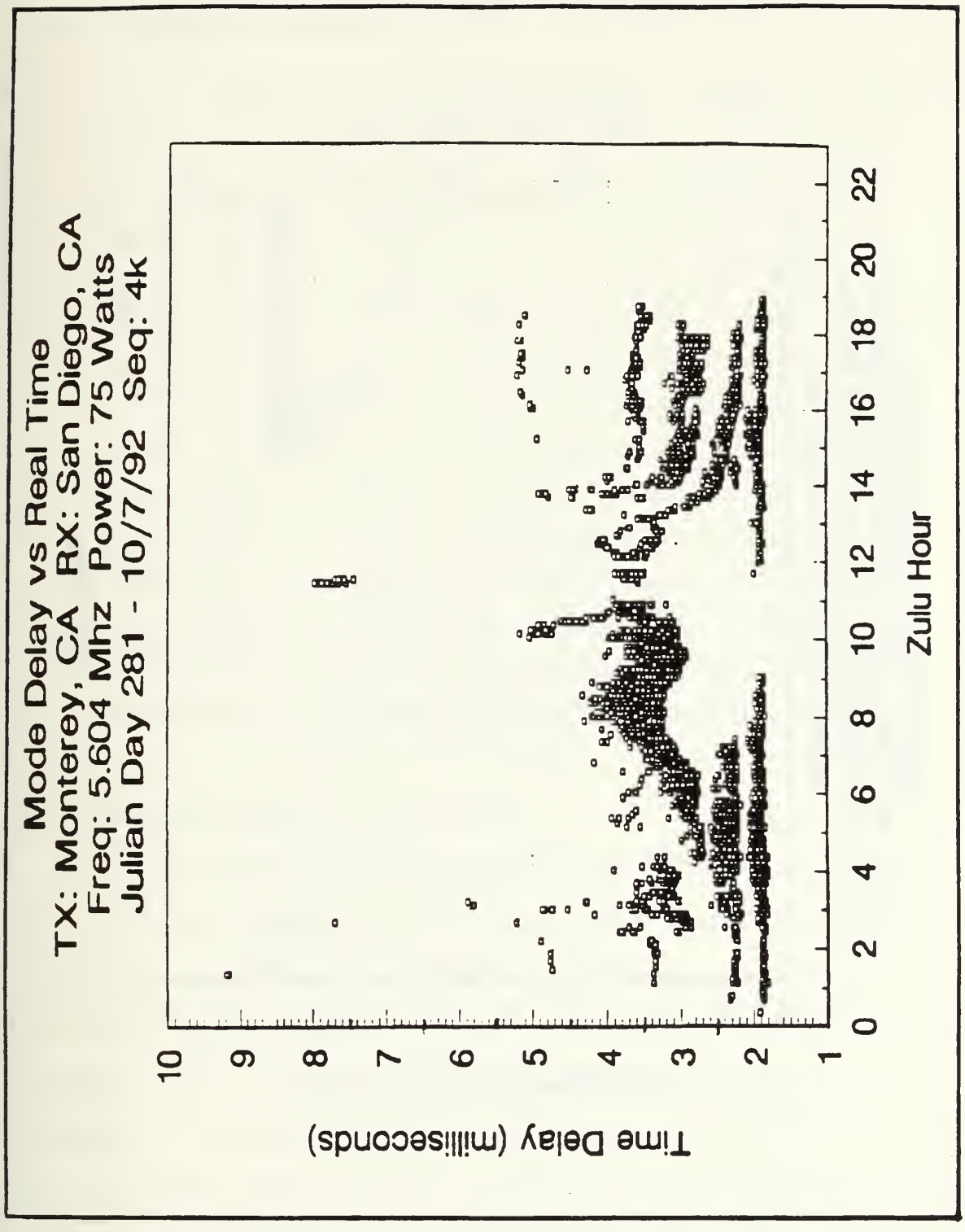

Figure 16. Measured Mode Delay for 7 Oct 92.

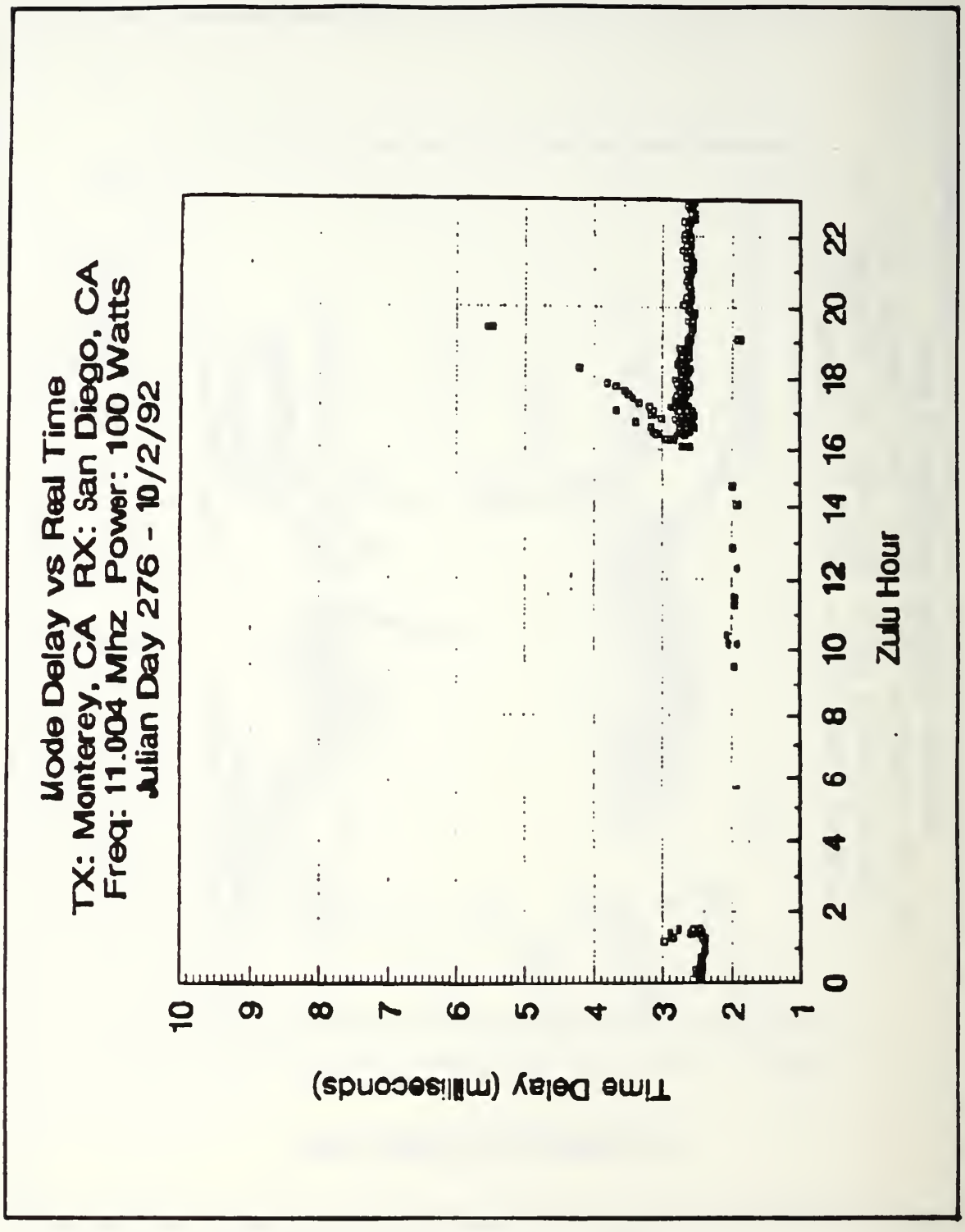

Figure 17. Measured Mode Delay for 2 Oct 92.
(11.004 MHz - 100 watts)

correspondence between GMT and link local time.

TABLE 2. TIME CORRESPONDENCE BETWEEN GMT AND LOCAL TIME

GMT	Local Time	GMT	Local Time
00:00	16:00	12:00	04:00
01:00	17:00	13:00	05:00
02:00	18:00	14:00	06:00
03:00	19:00	15:00	07:00
04:00	20:00	16:00	08:00
05:00	21:00	17:00	09:00
06:00	22:00	18:00	10:00
07:00	23:00	19:00	11:00
08:00	00:00	20:00	12:00
09:00	01:00	21:00	13:00
10:00	02:00	22:00	14:00
11:00	03:00	23:00	15:00

B. ADVANCED PROPHET 4.3 RESULTS

1. Input Scenario Parameters for PROPHET

In order to have a controlled experiment and a basis for comparison between experimental and computer predicted data, an environment similar to the experimental scenario was created. The first step in using ADVANCED PROPHET 4.3 is to define the transmitter and receiver antenna characteristics and receiving site noise. As mentioned in Chapter III the radiation patterns for both antennas were obtained via NEC simulation. Man-made noise was defined as QM-type (quasi-minimum). The 10.7 cm. solar radio flux as well as Kp (the

planetary magnetic index) were provided by Mr. Wayne Bratt of the Naval Research and Development Center (NRAD) San Diego, shown in Table 3. Since Kp is an average of the variation of

TABLE 3. MAGNETIC INDEX AND 10.7 cm. SOLAR RADIO FLUX USED IN PROPHET SIMULATIONS.

Date	10.7 cm. Flux	Magnetic Index (Kp)
28 Aug 92	96	2 2 1 1 2 2 1 1
02 Oct 92	118	4 6 4 4 3 2 3 2
03 Oct 92	120	1 2 2 2 2 3 3 2
04 Oct 92	120	1 2 2 2 2 3 3 2
07 Oct 92	137	3 3 1 2 3 2 2 1

the magnetic field on the earth over a three-hour period, eight (8) constants for each day were divided in three hours intervals. RAYTRACE, a program that is part of ADVANCED PROPHET 4.3, was used to obtain the different time delays for the Monterey-San Diego communications link. This program calculates ray paths that propagate between the transmitter and receiver antennas for a given frequency, time and ionospheric parameters. These calculations are controlled by input parameters such as launch angle, from which the initial, increment and maximum launch angles are used to compute all possible ray paths. RAYTRACE "shoots" rays from the transmitter and notes where each one "lands" in the vicinity of the receiver. The two closest-landing rays are noted and the ray which completes the path is calculated by interpolation of nearby ray paths. The resulting ray is called

a mode. The launch angle is then increased until a second mode is obtained. The calculation process terminates when one of the following conditions is met:

* The initial ray does not bounce off the ionosphere but rather penetrates it.
* The launch angle reaches the maximum specified value.
* The maximum number of modes are reached by the program itself.

The user in ADVANCED PROPHET can define ionospheric parameters such as:

* Critical frequency of the E-region (foE).
* foEs if the Sporadic E-layer is to be considered.
* Critical frequency of the F1 region, foF1.
* Critical frequency of the F2 region, foF2.
* F2-layer maximum density altitude, hmF2.
* F2-layer semi-thickness, YmF2.

When these parameters are specified, the ionosphere will be assumed to be uniform throughout the region of propagation. If these parameters are not user specified, ADVANCED PROPHET uses internal models to calculate the parameters including variations along the path due to time of day, solar activity and the link geographical region [5].

2. ADVANCED PROPHET 4.3 Data Analysis

After all calculations are completed, two types of output displays are generated. The first type of display shows the parameters which defined the calculations and the

plots of the rays paths, as shown in Figure 18. The second display details the results of the calculations in alphanumerical fashion, as seen in Figure 19. For the comparison process, the rubric, or unique descriptor, corresponding to the mode delay (msec) was used to identify the different mode path geometries; this delay is the total calculated group delay.

To consider a propagation mode delay prediction valid for the comparison, the signal to noise ratio (SNR) should be greater than 0 dB. From the alphanumeric output of the Raytrace program the SNR can be determined for each of the propagation mode delays. The other rubrics of the display lists calculated propagation modes, such as number of hops, ionospheric bounce region and trajectory losses. For the analysis, data obtained from RAYTRACE alphanumeric output were utilized.

C. DATA COMPARISON

Figures 20 through 25 show experimental and ADVANCED PROPHET 4.3 generated mode delay data. Data plotted for a given day were assigned "o" and "x" corresponding to PROPHET and experimental data respectively. There is a similarity between the data, especially in the 2 - 7 msec time frame. PROPHET predicts mode delays that are greater than 15 msec, which are not observed in the experiment. In addition, PROPHET shows increasing mode delays for the first six hours of the day, 0000 through 0600 GMT (1600 through 2200, the

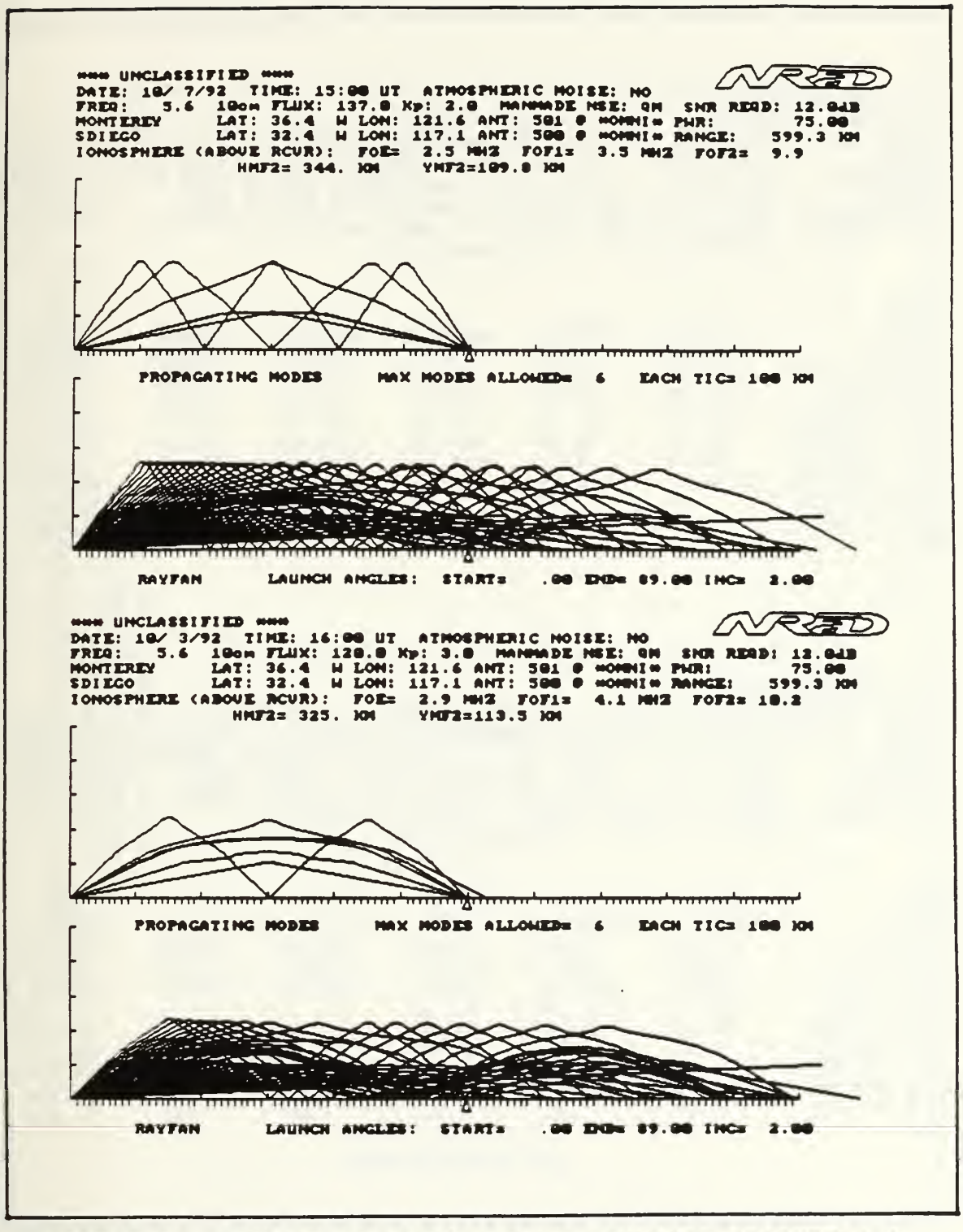

Figure 18. Ray Paths predicted by ADVANCED PROPHET 4.3

```
*** UNCLASSIFIED ***
RAYTRACE SYNOPSIS -- LAUNCH ANGLES: START=   .00 END= 89.00 INC=  2.00
DATE: 10/ 7/92 TIME: 15:00 UT  ATMOSPHERIC NOISE: NO  BWIDTH:  1.240 KHZ
FREQ:   5.6  10cm FLUX: 137.0 Kp: 2.0  MANMADE NSE: QM  SNR REQD: 12.0dB
MONTEREY     LAT: 36.4  W LON: 121.6 ANT: 501 @ *OMNI* PWR:       75.00
SDIEGO       LAT: 32.4  W LON: 117.1 ANT: 500 @ *OMNI* RANGE:   599.3 KM
IONOSPHERE:  FOE=  2.5 MHZ  FOF1=  3.5 MHZ  FOF2=  9.9
             HMF2= 344. KM    YMF2=109.8 KM


NHOP             1         1         1         1         2         3
MODE       1000000   1000000   1000000   3000000   3300000   3330000
ANGLE        18.65     23.50     23.90     45.35     62.45     70.80
DELAY(MSEC)  2.147     2.233     2.247     2.969     4.509     6.354
LOSS(DB)     127.29    147.35    169.46    120.01    128.06    138.42
GAIN  TX/RX  -4/ -3    -2/  0    -1/  0    1/  3    1/  4    1/  4
1HZ SNR(DB)   49.66     34.04     12.24     66.52     60.37     49.94
ADJ SNR(DB)   18.73      3.11    -18.70     35.59     29.43     19.00
VIR HT1(KM)  110.11    140.86    143.92    326.29    303.14    302.23
VIR HT2(KM)     .00       .00       .00       .00    302.03    302.66
VIR HT3(KM)     .00       .00       .00       .00       .00    300.04
RA>



*** UNCLASSIFIED ***
RAYTRACE SYNOPSIS -- LAUNCH ANGLES: START=   .00 END= 89.00 INC=  2.00
DATE: 10/ 3/92 TIME: 16:00 UT  ATMOSPHERIC NOISE: NO  BWIDTH:  1.240 KHZ
FREQ:   5.6  10cm FLUX: 120.0 Kp: 3.0  MANMADE NSE: QM  SNR REQD: 12.0dB
MONTEREY     LAT: 36.4  W LON: 121.6 ANT: 501 @ *OMNI* PWR:       75.00
SDIEGO       LAT: 32.4  W LON: 117.1 ANT: 500 @ *OMNI* RANGE:   599.3 KM
IONOSPHERE:  FOE=  2.9 MHZ  FOF1=  4.1 MHZ  FOF2= 10.2
             HMF2= 325. KM    YMF2=113.5 KM


NHOP             1         1         1         1         1         2
MODE       1000000   2000000   2000000   2000000   3000000   3300000
ANGLE        17.95     29.95     43.65     44.85     48.10     62.05
DELAY(MSEC)  2.135     2.364     2.873     3.067     3.122     4.438
LOSS(DB)     140.94    135.84    135.38    176.66    129.37    137.59
GAIN  TX/RX  -4/ -3     0/  2     0/  2     1/  3     1/  3     1/  4
1HZ SNR(DB)   35.25     49.14     50.80      9.77     57.66     50.82
ADJ SNR(DB)    4.31     18.21     19.87    -21.17     26.72     19.89
VIR HT1(KM)  105.79    184.70    307.93    336.69    360.24    299.27
VIR HT2(KM)     .00       .00       .00       .00       .00    295.23
VIR HT3(KM)     .00       .00       .00       .00       .00       .00
RA>
```

Figure 19. Alphanumeric output corresponding to Raytrace predictions.

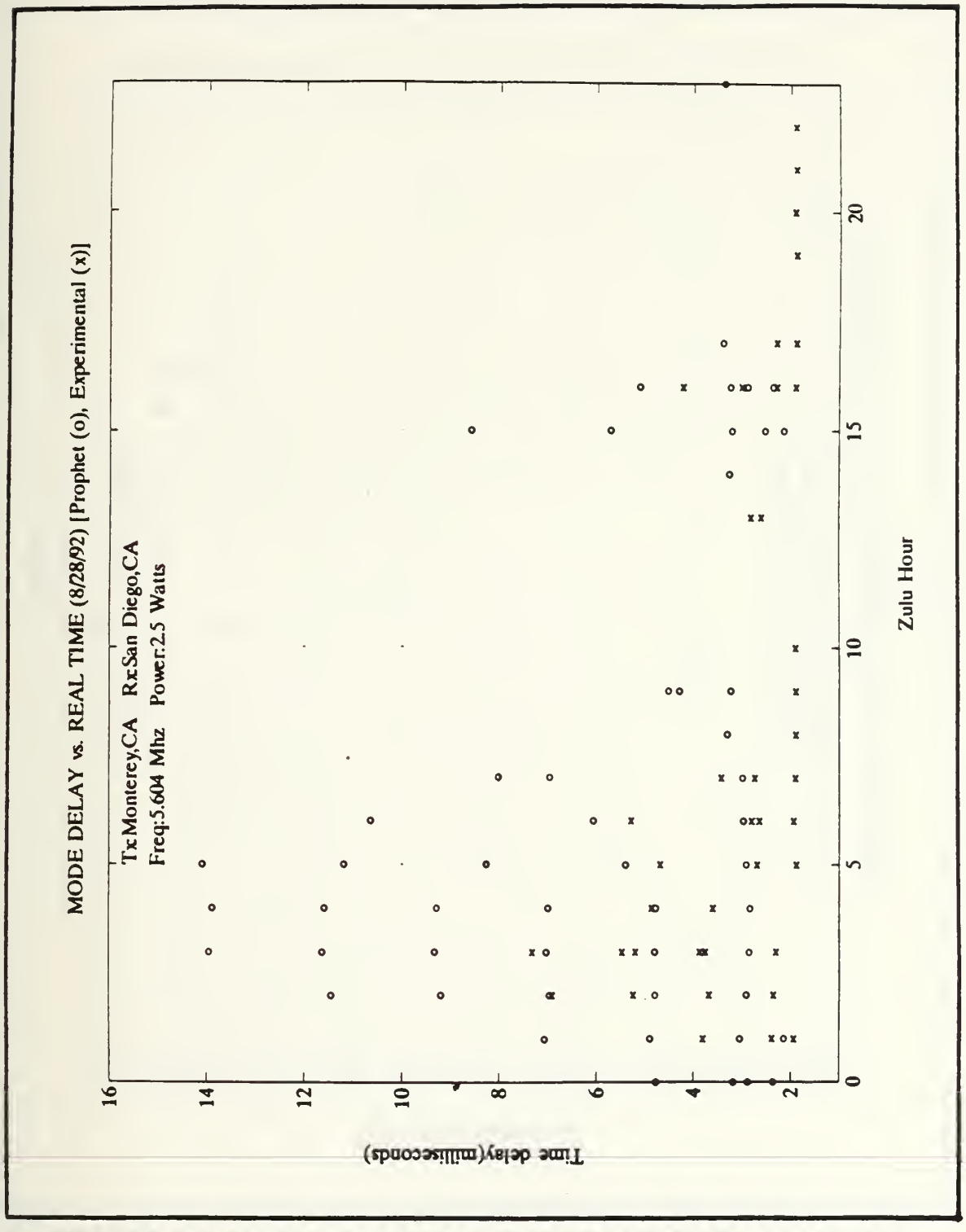

Figure 20. Comparison between experimental and PROPHET Mode Delay predictions for 28 Aug 92.

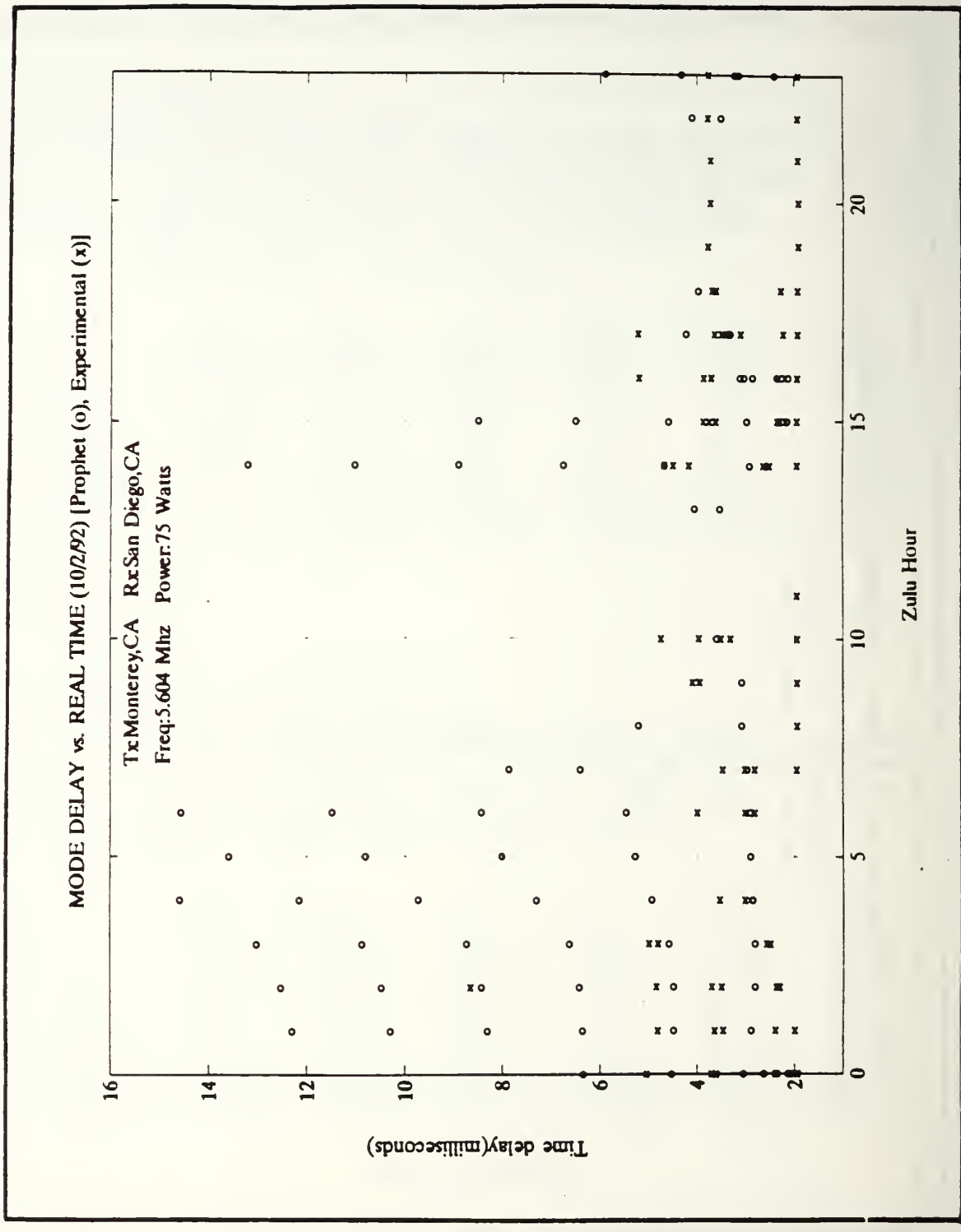

Figure 21. Comparison between experimental and PROPHET Mode Delay predictions for 2 Oct 92. (5.604 - 75 watts).

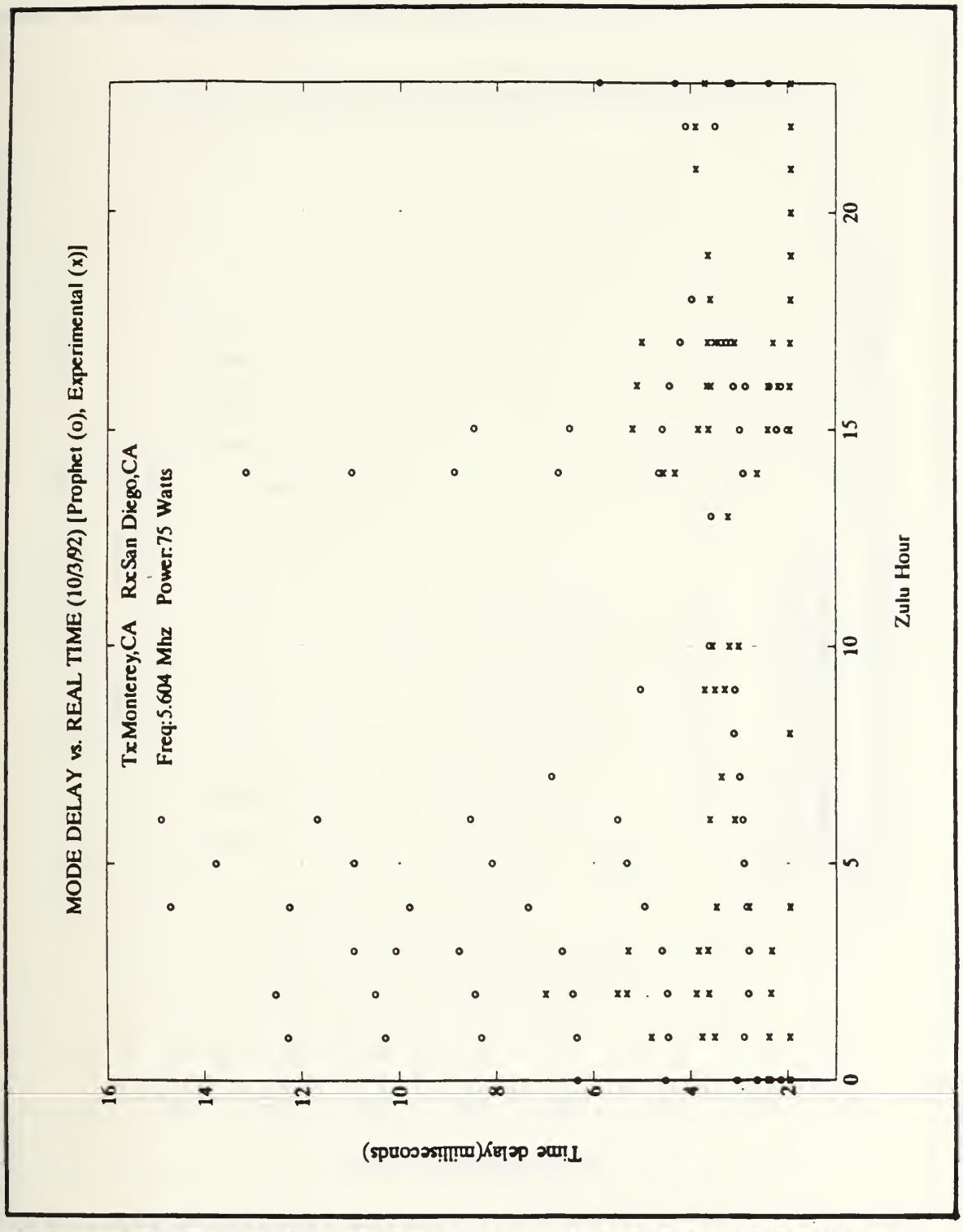

Figure 22. Comparison between experimental and PROPHET Mode Delay predictions for 3 Oct 92.

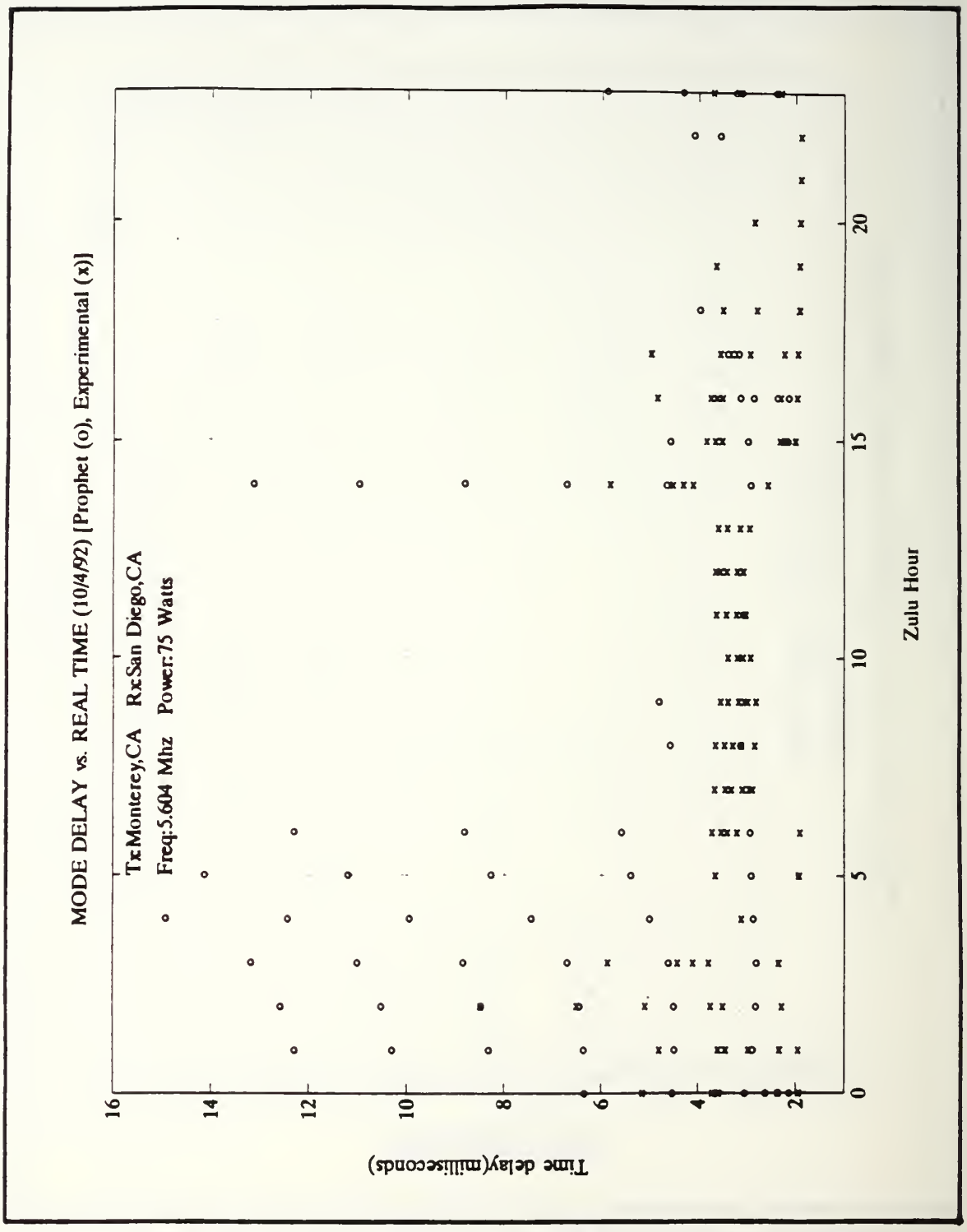

Figure 23. Comparison between experimental and PROPHET Mode Delay predictions for 4 Oct 92.

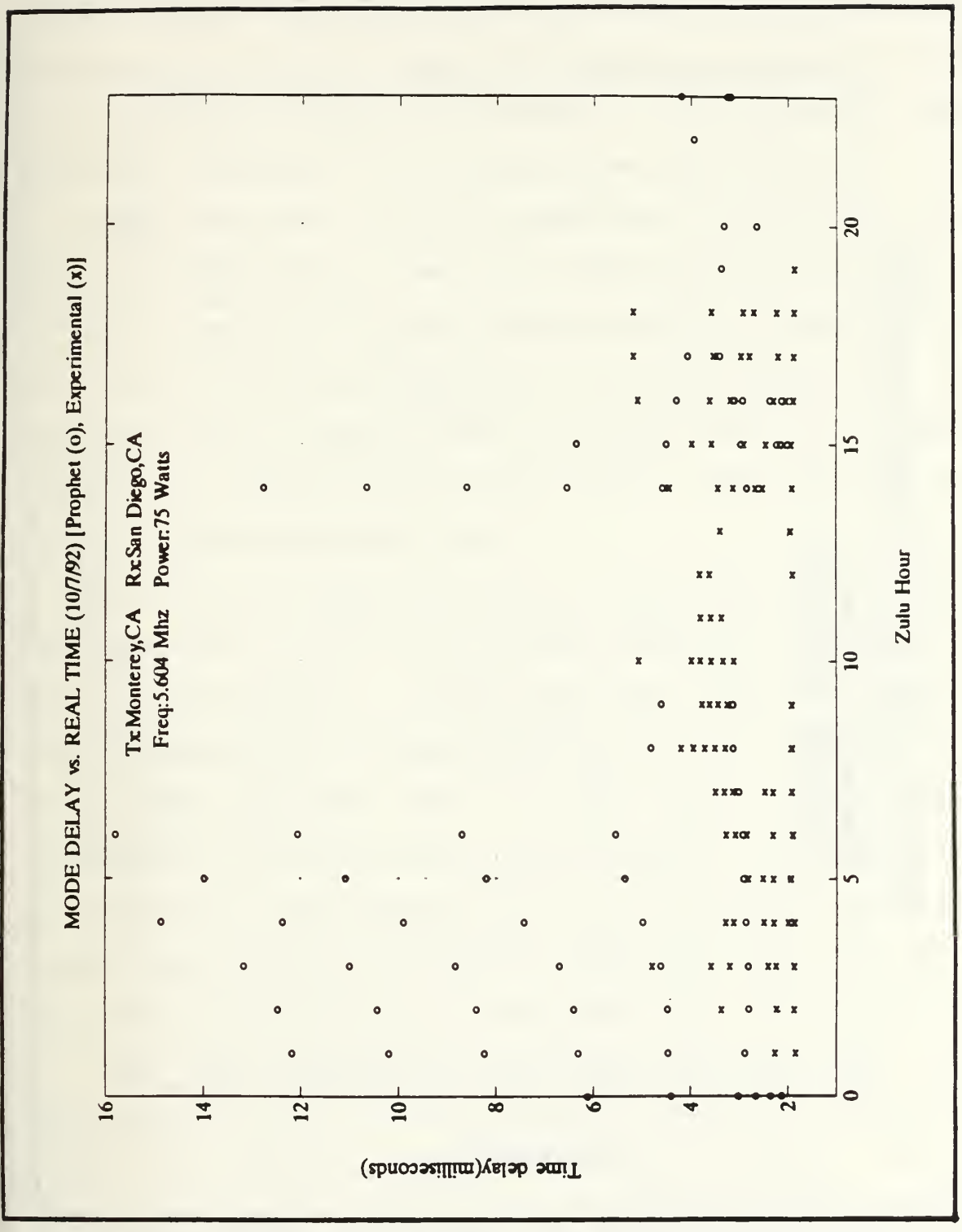

Figure 24. Comparison between experimental and PROPHET Mode Delay predictions for 7 Oct 92.

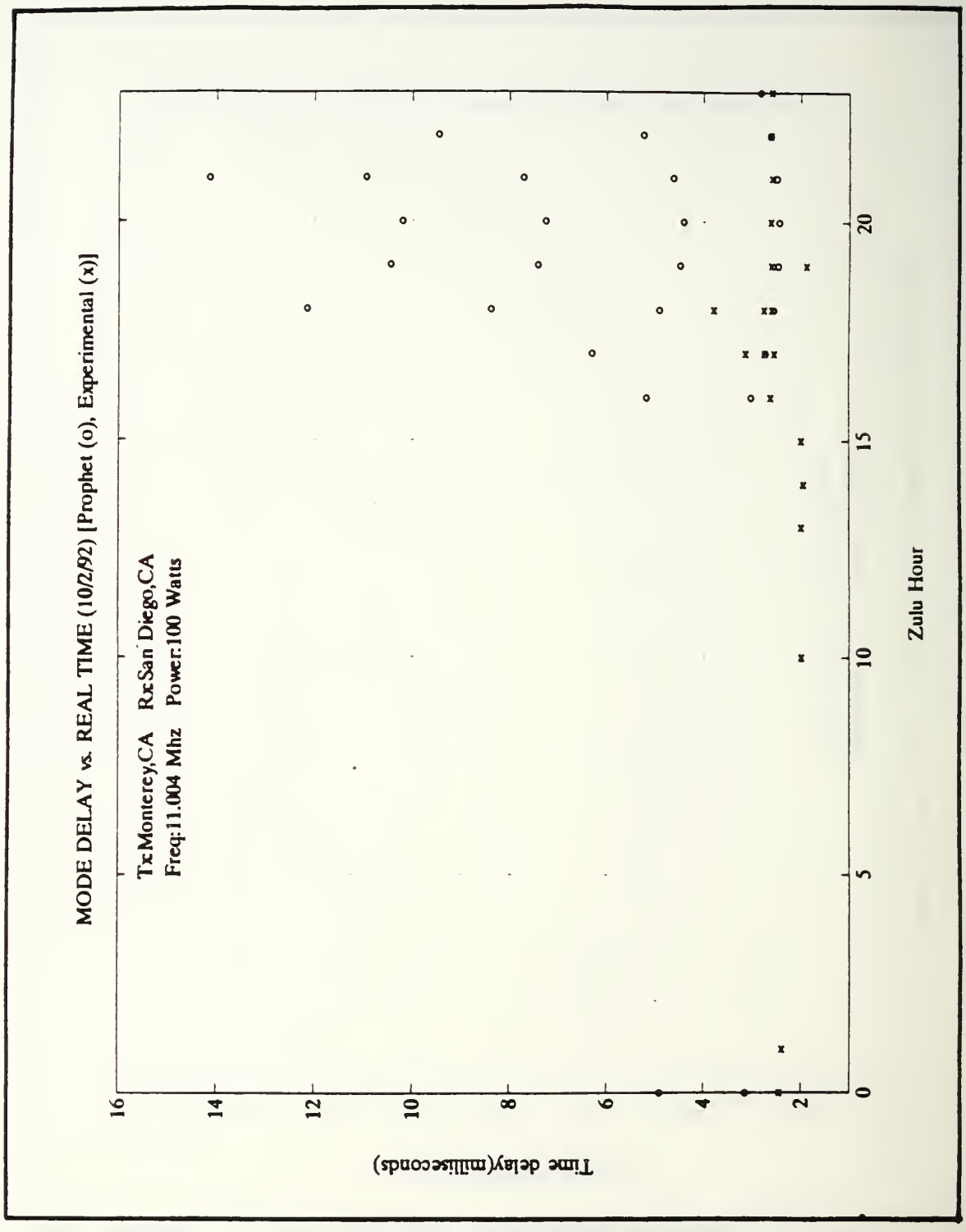

Figure 25. Comparison between experimental and PROPHET Mode Delay predictions for 2 Oct 92. (11.004 - 100 watts).

local time for San Diego), which is similar in some aspects to experimental results. Single and multihop propagation of up to six hops are predicted by PROPHET. The experimental data plotted in Figures 12 to 16 shows only three modes.

In Figure 25 for 2 Oct 92, PROPHET data obtained at 11.004 MHz with 100 watts is close to the experimental data, where in the early hours of the day, propagation is not supported by the path. Good correspondence between experimental and PROPHET data is noted between 1600 and 2400 GMT. ADVANCED PROPHET 4.3 predicts mode delays above 4 msec that are not shown in the experimental data.

For further comparison between experimental and PROPHET data, an hour by hour, day by day breakdown is provided in Figures 26 through 31. These plots were created by counting the times for which the experimental and predicted delays were a different by less than 0.5 msec. All hours in which propagation for both cases was not available are marked with an asterisk. From Figures 26 to 31 it is seen that maximum correlation between PROPHET and experimental data occurs in the early hours of the day and between 1400 and 1900 GMT.

The third comparison was calculation of the total percentage per hour, over the five day period, in which the time delay differences were less than 0.5 msec. In this manner a global comparison is performed to more fully appreciate how the percentages are distributed throughout the day. Table 4 and Figure 32 show this comparison. All of the

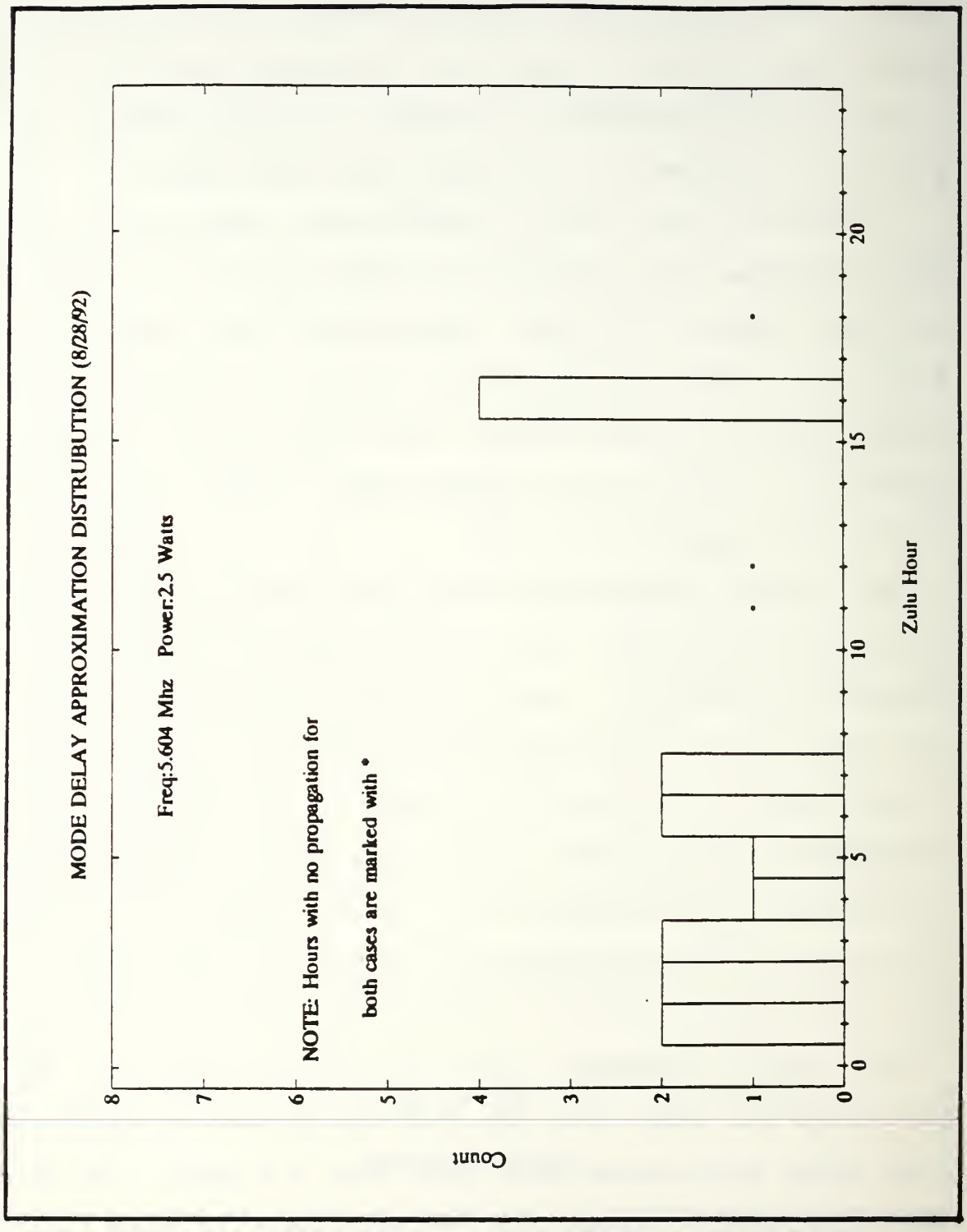

Figure 26. Mode Delay Approximation Distribution for 28 Aug 92

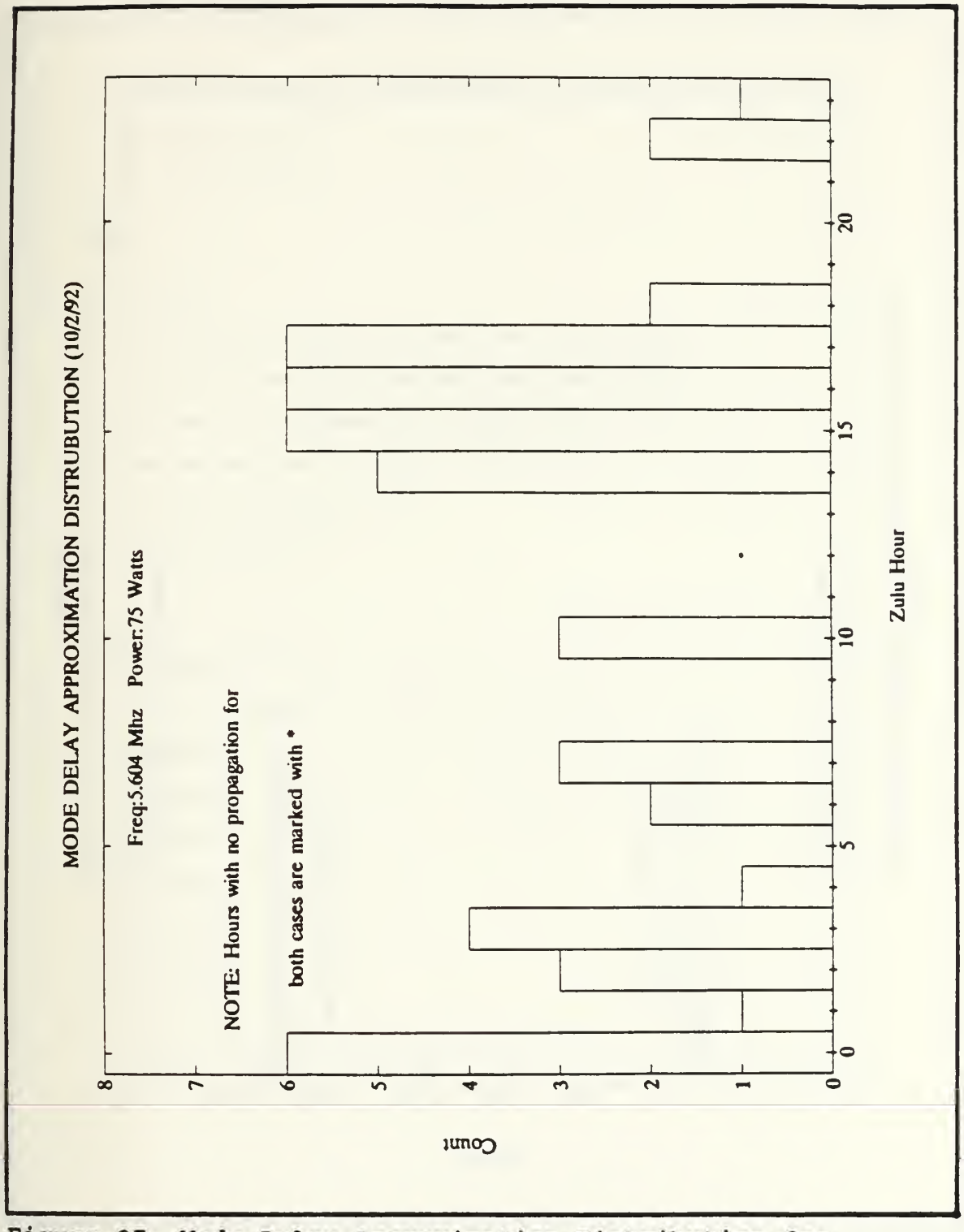

Figure 27. Mode Delay Approximation Distribution for 2 Oct 92 (5.604 MHz - 75 watts)

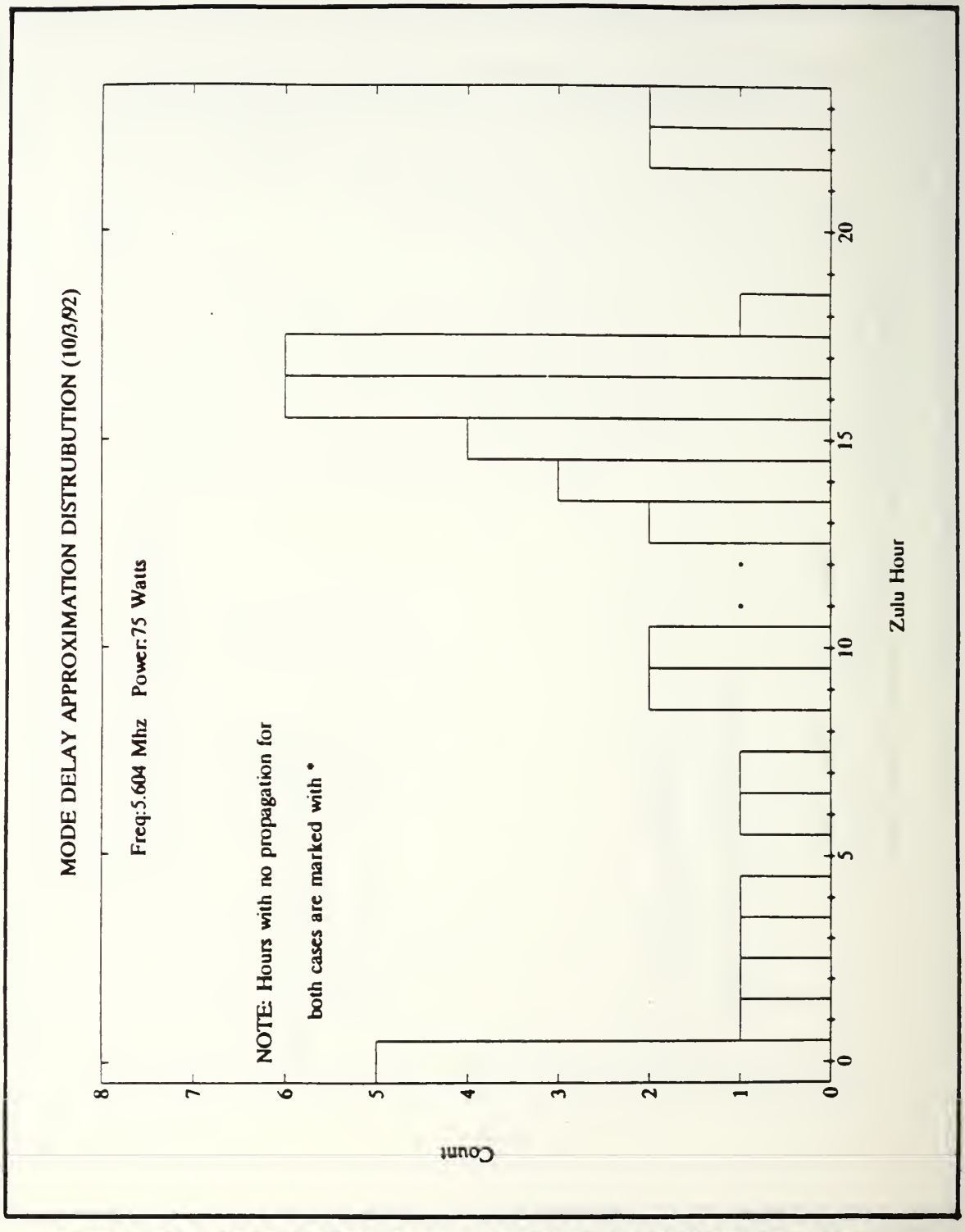

Figure 28. Mode Delay Approximation Distribution for 3 Oct 92

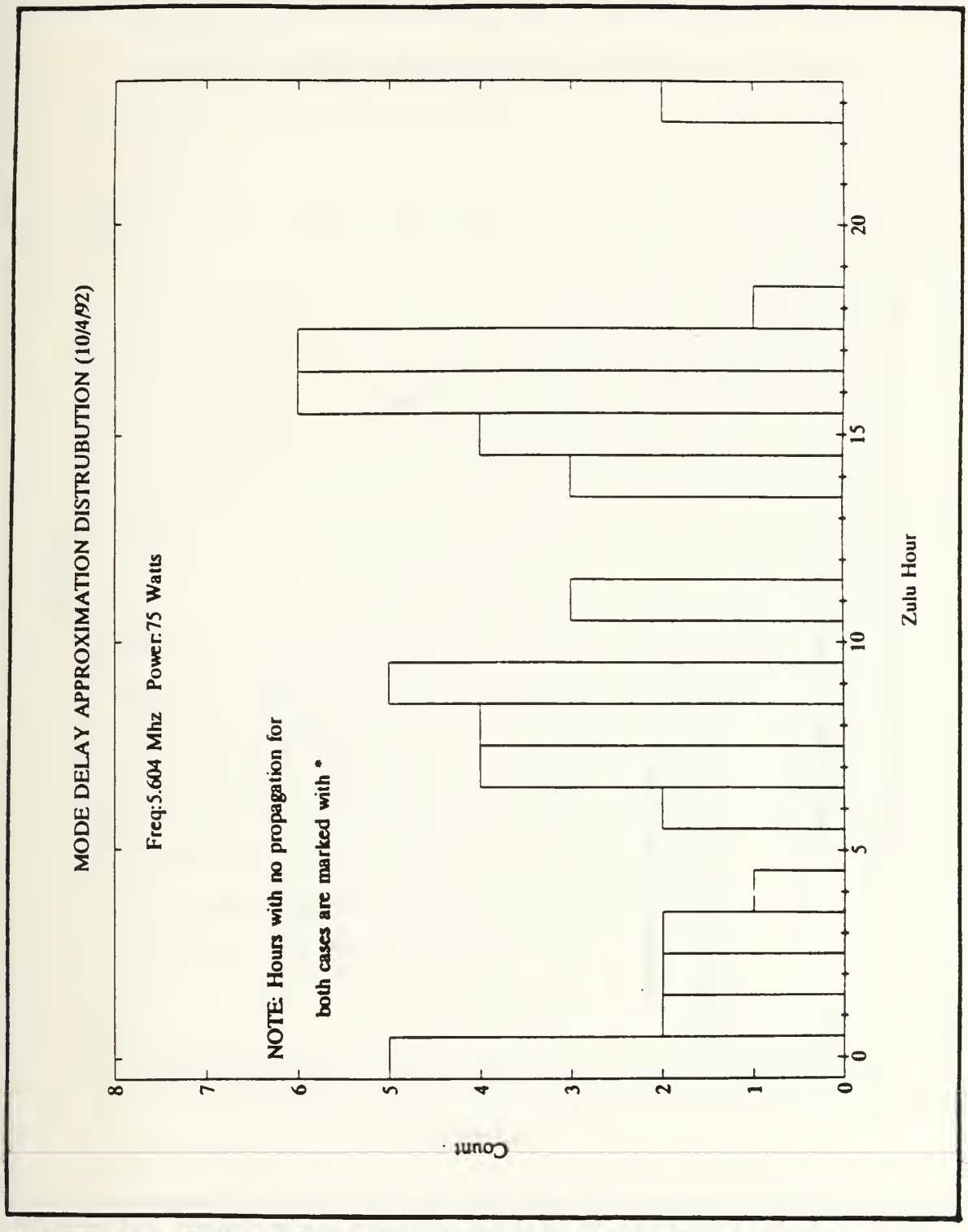

Figure 29. Mode Delay Approximation Distribution for 4 Oct 92

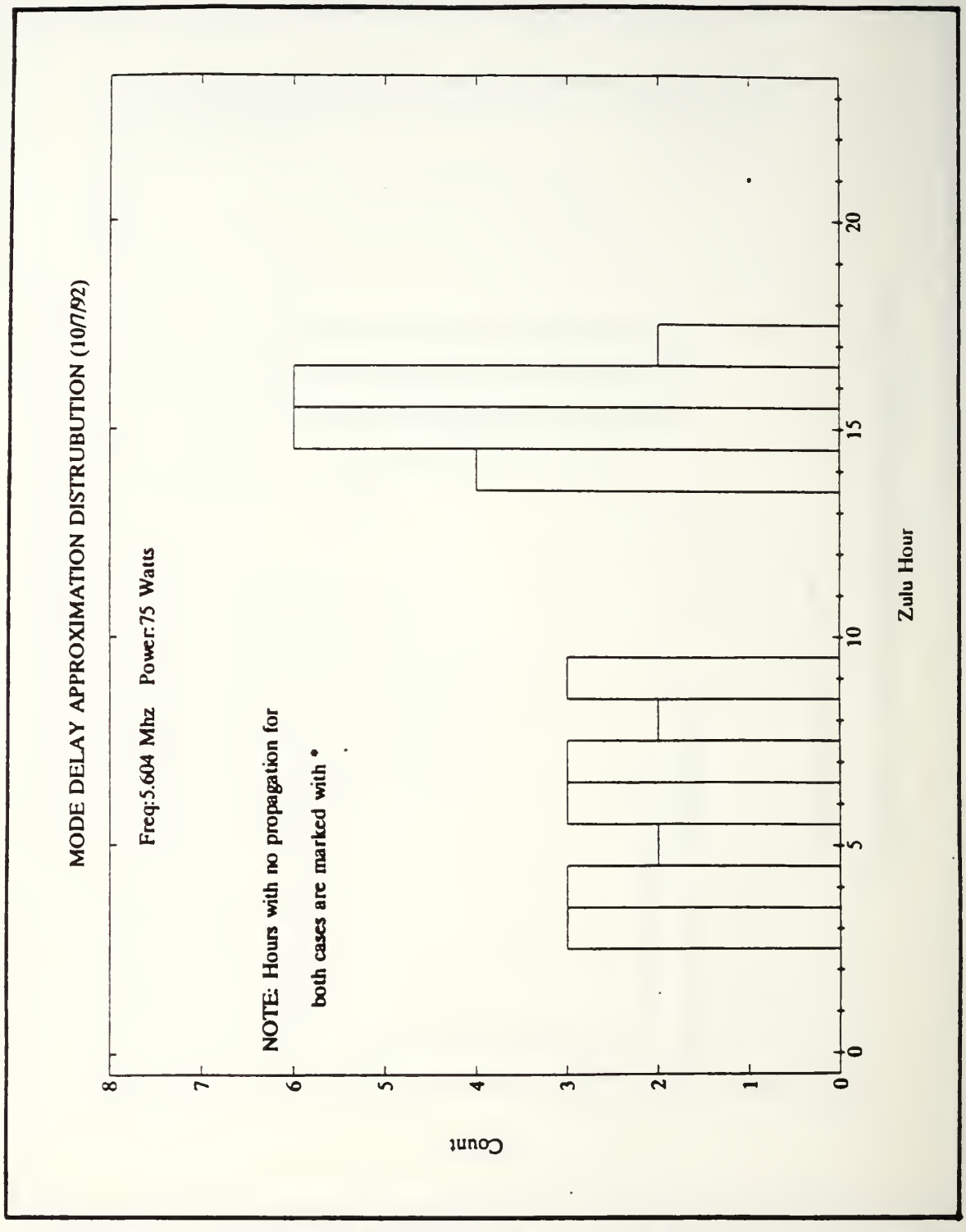

Figure 30. Mode Delay Approximation Distribution for 7 Oct 92

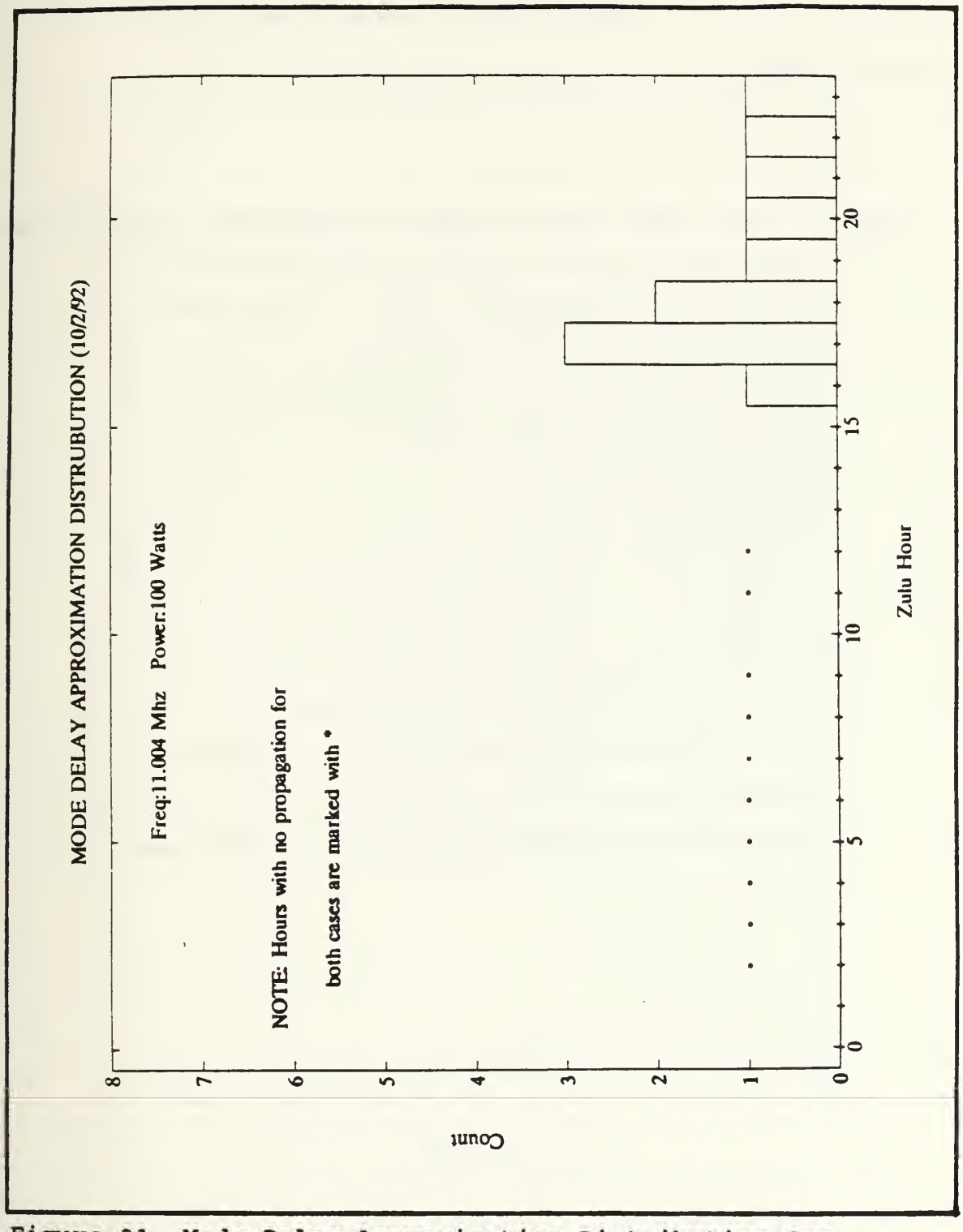

Figure 31. Mode Delay Approximation Distribution for 2 Oct 92 (11.004 MHz - 100 watts)

comparisons and plotted results were made with the aid of MATLAB programs.

TABLE 4. MODE DELAY APPROXIMATION PERCENTAGE DISTRIBUTION

GMT	Percentage	GMT	Percentage
00:00	7.143	12:00	1.786
01:00	2.679	13:00	0.893
02:00	4.018	14:00	6.696
03:00	5.804	15:00	8.929
04:00	3.571	16:00	12.946
05:00	1.786	17:00	10.268
06:00	4.911	18:00	2.678
07:00	6.250	19:00	0.446
08:00	3.125	20:00	0.446
09:00	4.911	21:00	0.893
10:00	2.232	22:00	2.232
11:00	2.679	23:00	2.678

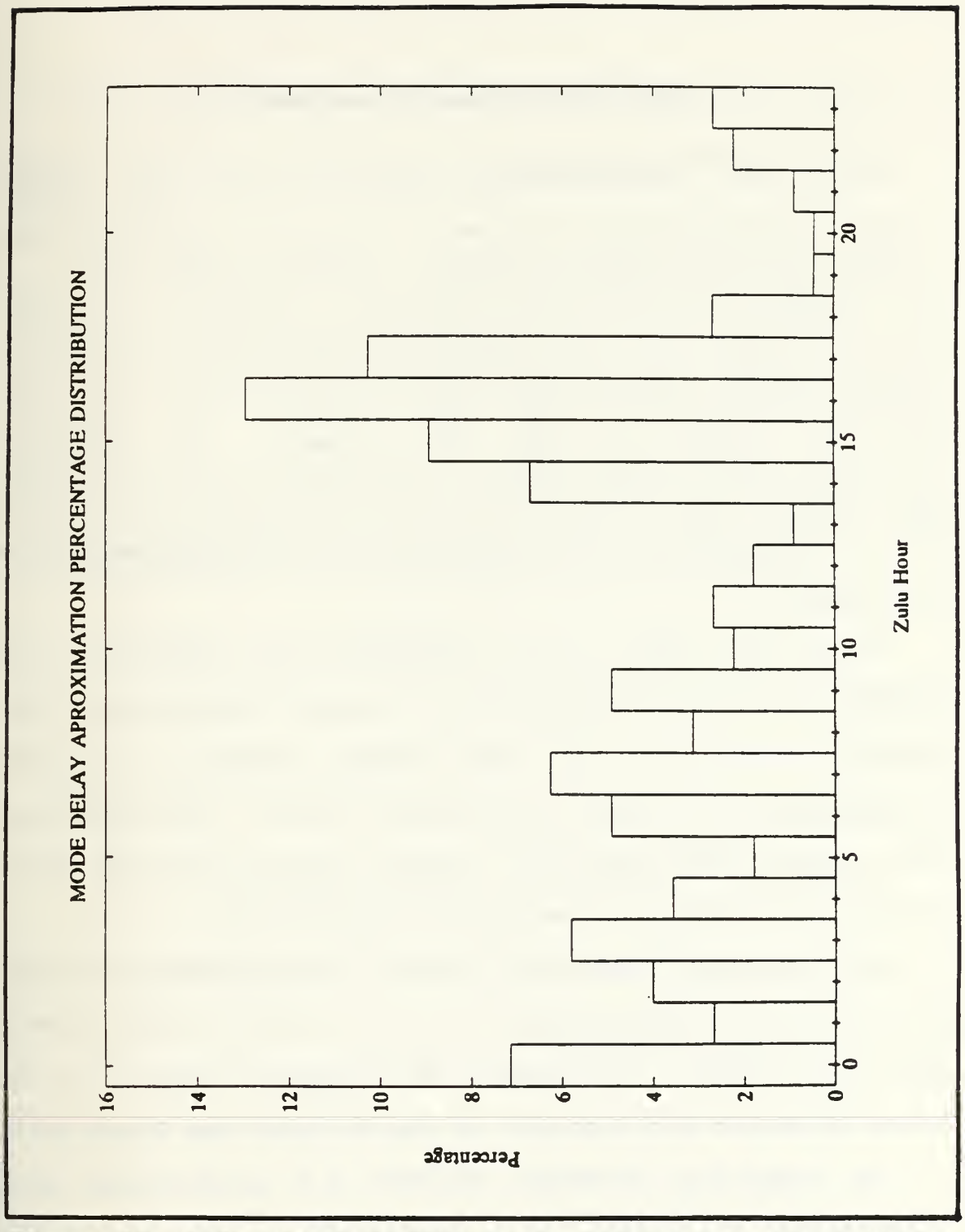

Figure 32. Mode Delay approximation percentage distribution.

V. CONCLUSIONS AND RECOMMENDATIONS

The field measurements indicate that the PROPHET propagation predictions are most accurate for the early hours of 1400 until 1700 GMT of each day. Data taken on 2 Oct 92 at 11.004 MHz show that when skywave propagation is supported, the experimental and program predictions are almost identical, for mode delays of less than 4 msec. As expected, experimental and program results are similar also for the part of the day when skywave propagation is not supported by the ionosphere.

Field data taken at 5.6 MHz showed good agreement with PROPHET propagation predictions. Between 0000 and 0600 GMT, PROPHET predicted six mode delay groups (multi-hop propagation) with delays that exceed 15 msec. This same trend was observed experimentally; however, only three mode delay groups were present between 0000 and 0400 GMT.

It can be concluded that the best correspondence between predictions and measurements occurs at 0000 GMT and between 1400 and 1700 GMT. Reasonable correspondence occurs for the hours of sunset and midnight on the Monterey-San Diego path.

In comparing ADVANCED PROPHET 4.3 predictions with experimental field data, it is preferable to input the values of the required ionospheric variables corresponding to the time the measurements were taken. Since these values were not

available for the data used in this research, approximate values based on PROPHET's internally generated parameter set were used.

More data is needed, covering the entire HF band, and will be collected as the equipment and software are refined. Once the questionable CCIR recommendations for measuring signal strength are resolved, SNR can be measured by standard procedures and compared with PROPHET predictions. Additional ionospheric propagation software such as IONCAP, ICEPAC, ASAPS and AMBCOM should be evaluated along with PROPHET.

LIST OF REFERENCES

1. Leon F. McNamara, **The Ionosphere: Communications, Surveillance, and Direction Finding**. Krieger Publishing Company, Malabar, Florida, 1991.
2. Kenneth Davies, **Ionospheric Radio Waves**. Blaisdell Publishing Company, 1969.
3. Yakov L. Al'pert, **Radio Wave Propagation and the Ionosphere V.1.** Consultans Bureau, New York, 1973.
4. Nicholas M. Maslin, **HF Communications: A Systems Approach.** Plenum Press, New York, 1987.
5. **Operator's Manual for the ADVANCED PROPHET System.** Delfin Systems, Sunnyvale, California, 1991.
6. Gerhard Braun, **Planning and Engineering of Short Wave Links**, Siemens, Berlin, 1986.
7. Jeffrey J. Burtch, **A Comparison of High-Latitude Ionospheric Propagation Predictions from ICEPAC with Measured Data**, Master's thesis, Naval Postgraduate School, Monterey, CA, September 1991.
8. David J. Wilson, **A Comparison of High-Latitude Ionospheric Propagation Predictions from AMBCOM with Measured Data**, Master's thesis, Naval Postgraduate School, Monterey, CA, March 1991.
9. Stefanos S. Gikas, **A Comparison of High-Latitude Ionospheric Propagation Predictions from ADVANCED PROPHET**

4.0 with Measured Data, Master's thesis, Naval Postgraduate School, Monterey, CA, December 1990.

INITIAL DISTRIBUTION LIST

		No Copies
1.	Defense Technical Information Center Cameron Station Alexandria, VA 223004-6145	2
2.	Library, Code 52 Naval Postgraduate School Monterey, CA 93943-5002	2
3.	Chairman, Code EC Department of Electrical and Computer Engineering Naval Postgraduate School Monterey, CA 93943	1
4.	Professor R. W. Adler, Code EC/Ab Department of Electrical and Computer Engineering Naval Postgraduate School Monterey, CA 93943	3
5.	Professor Donald van Z. Wadsworth, Code EC/Wd Department of Electrical and Computer Engineering Naval Postgraduate School Monterey, CA 93943	1
6.	Dr. James K. Breakall Penn State University 306 EE East University Park, PA 16802	1
7.	Nate C. Gerson 877 Oakdale Circle Millersville, MD 21108	1
8.	Dr. Robert Hunsucker R P Consultants 1618 Scenic Loop Fairbanks, AK 99709	1
9.	George Lane Voice of America/ESBA 300 Independence Ave. SW Washington, DC 20547	1
10.	Jane Perry 1921 Hopefield Rd Silver Spring, MD 20904	1

11. Robert M. Rose 1
Naval Ocean Systems Center, Code 542
San Diego, CA 92152-5000